https://dx.doi.org/10.1016/j.advengsoft.2018.04.003

ErosLab: A modelling tool for soil tests

Yin-Fu JIN[1,2] and Zhen-Yu YIN[1,2,*]

Affiliation:

1 Research Institute of Civil Engineering and Mechanics (GeM), UMR CNRS 6183, Ecole Centrale de Nantes, France

2 Key Laboratory of Geotechnical and Underground Engineering of Ministry of Education; Department of Geotechnical Engineering, College of Civil Engineering, Tongji University, Shanghai, China, 200092

* Corresponding author: Dr Zhen-Yu YIN, Tel: +33 (0)240371588 / Fax: +33 (0)240372535; E-mail: zhenyu.yin@gmail.com

Abstract: The focus of this paper is ErosLab, a useful tool for the development, analysis and application of constitutive models developed to solve the modelling problems inherent in soil tests. The ErosLab is programmed in the way of admixture programming with C#, MATLAB and FORTRAN, offering a powerful environment for various kinds of modelling soil tests. The proposed tool has six important features: (1) a mechanical calculator; (2) the ability to cover various kinds of soil tests; (3) a number of soil models with a user extension interface; (4) multiple methods of loading control; (5) comprehensive and efficient debugging; and (6) visualisation with graphical displays. Furthermore, the entire graphical user interface and usage instructions for the tool are briefly illustrated in simple and practical terms. Finally, three case studies are presented in which ErosLab was used, to highlight its performance in modelling tests for different soils.

Key words: laboratory tests; geomechanics; geotechnical engineering; constitutive model; interface; software

1 Introduction

Constitutive models play an important role in the design and construction of geotechnical engineering. To date, hundreds of different soil constitutive models, varying in view from micro to macro, have been proposed [1-10]. A range of results may be obtained depending on the selection of model, leading to different engineering decisions, which consequently alters the economy and risk level of problems. However, most engineers have failed to fully understand constitutive models and have invariably chosen a model based on their own preferences and experiences, hoping that a "one-size-fits-all" approach can solve all engineering problems. Some widely used models can sometimes result in significantly unreasonable predictions when applying to conventional engineering [11], as seen when the Mohr-Coulomb model was adopted to analyse an excavation [12] and when the modified cam-clay was employed to predict the long-term settlement of embankment [13-16]. A lack of proper understanding of the constitutive model has become one of the main risk factors in terms of accidents [17-21]. Therefore, it is essential that the merits and drawbacks of the selected model are completely understood before its application. In general, the quickest way to do this is to simulate laboratory tests. However, most engineers struggle with writing a computer program that can implement the soil model to achieve such a simulation. To address this, a tool that could model soil tests by providing a variety of constitutive models would be highly useful.

Previously, a range of practical tools in the field of geotechnical engineering have been developed. These offer an object-oriented design to simulate engineering issues using a variety of constitutive models, such as some commercial codes (ABAQUS[22], FLAC[23], PLAXIS[24] and COMSOL[25]), or open sources codes [26-29]. Of these, only PLAXIS has partial functions in the modelling of soil tests. However, the kinds of tests provided, and the loading control, are somewhat limited. This bolsters the case for the development of a tool that can offer a powerful environment for simulating various kinds of laboratory tests. Engineers could use this to understand a soil model without the need to reproduce its mode of operation, which is another area of difficulty.

In this paper, a modelling tool (ErosLab) for soil laboratory tests is developed and introduced. First, the different kinds of tests that can be used with the tool are briefly introduced. Second, its

general framework is presented, including its mixed language programming and six main features. Third, its graphical user interface and usage instructions are illustrated. Finally, descriptions are given of the carrying out of three cases of parameter identification (first for modelling of sand behaviours, second for modelling of clay behaviours and the third for modelling of time effects of soil). The developed software can be freely downloaded from the following URL: http://www.geoinvention.com/en/news.asp?big=14.

Since the development of constitutive models is usually based on laboratory tests, developing this tool should be first helpful for the research purpose of constitutive modelling. Even though field-scale problems cannot be directly simulated, the debugging scheme in this tool includes complex loading combinations reflecting various in-situ conditions. Furthermore, the tool should also be helpful for the teaching purpose and basic training of constitutive modelling for students.

2 Basic definitions

2.1 Stress analysis

The stress state of a single element can be described using six independent stress components. In constitutive model programming, the stress tensor is usually expressed as

$$\sigma_{ij} = \left[\sigma_{xx} \quad \sigma_{yy} \quad \sigma_{zz} \quad \sigma_{xy} \quad \sigma_{xz} \quad \sigma_{yz}\right]^T \tag{1}$$

The σ_m (or p) is defined as the average normal stress or mean effective stress:

$$\sigma_m = \frac{1}{3}\left(\sigma_{xx} + \sigma_{yy} + \sigma_{zz}\right) \tag{2}$$

~~Then, the stress tensor can be transformed to:~~

~~$$\sigma_{ij} = \begin{bmatrix} \sigma_{xx} - \sigma_m & \tau_{xy} & \tau_{xz} \\ \tau_{yx} & \sigma_{yy} - \sigma_m & \tau_{yz} \\ \tau_{zx} & \tau_{zy} & \sigma_{zz} - \sigma_m \end{bmatrix} + \begin{bmatrix} \sigma_m & 0 & 0 \\ 0 & \sigma_m & 0 \\ 0 & 0 & \sigma_m \end{bmatrix} \tag{3}$$~~

~~The first tensor in the equation is called the deviatoric stress tensor, while the second is termed the spherical stress tensor. The latter can be abbreviated to~~ $\sigma_m \delta_{ij}$ ~~or~~ $p\delta_{ij}$, ~~where~~ δ_{ij} ~~is the Kronecker symbol (~~ when $i = j$, $\delta_{ij} = 1$; when $i \neq j$, $\delta_{ij} = 0$ ~~).~~

The deviatoric stress tensor can be expressed as:

$$s_{ij} = \sigma_{ij} - \sigma_m \delta_{ij} = \begin{bmatrix} \sigma_{xx} - \sigma_m & \tau_{xy} & \tau_{xz} \\ \tau_{yx} & \sigma_{yy} - \sigma_m & \tau_{yz} \\ \tau_{zx} & \tau_{zy} & \sigma_{zz} - \sigma_m \end{bmatrix} = \begin{bmatrix} s_{xx} & s_{xy} & s_{xz} \\ s_{yx} & s_{yy} & s_{yz} \\ s_{zx} & s_{zy} & s_{zz} \end{bmatrix} = \begin{bmatrix} s_{11} & s_{12} & s_{13} \\ s_{21} & s_{22} & s_{23} \\ s_{31} & s_{32} & s_{33} \end{bmatrix} \tag{3}$$

The first, second and third invariants of the stress tensor are:

$$\begin{aligned} I_1 &= \sigma_{xx} + \sigma_{yy} + \sigma_{zz} \\ I_2 &= \begin{vmatrix} \sigma_{xx} & \tau_{xy} \\ \tau_{yx} & \sigma_{yy} \end{vmatrix} + \begin{vmatrix} \sigma_{yy} & \tau_{yz} \\ \tau_{zy} & \sigma_{zz} \end{vmatrix} + \begin{vmatrix} \sigma_{zz} & \tau_{zx} \\ \tau_{xz} & \sigma_{xx} \end{vmatrix} = \sigma_{xx}\sigma_{yy} + \sigma_{yy}\sigma_{zz} + \sigma_{zz}\sigma_{xx} - \tau_{xy}^2 - \tau_{yz}^2 - \tau_{zx}^2 \\ I_3 &= \begin{vmatrix} \sigma_{xx} & \tau_{xy} & \tau_{xz} \\ \tau_{yx} & \sigma_{yy} & \tau_{yz} \\ \tau_{zx} & \tau_{zy} & \sigma_{zz} \end{vmatrix} = \sigma_{xx}\sigma_{yy}\sigma_{zz} + 2\tau_{xy}\tau_{yz}\tau_{zx} - \sigma_{xx}\tau_{yz}^2 - \sigma_{yy}\tau_{zx}^2 - \sigma_{zz}\tau_{xy}^2 \end{aligned} \tag{4}$$

While the three invariants of the deviatoric stress tensor are:

$$\begin{cases} J_1 = s_{xx} + s_{yy} + s_{zz} = 0 \\ J_2 = \dfrac{1}{2} s_{ij} s_{ji} = \dfrac{1}{2}\left(s_{xx}^2 + s_{yy}^2 + s_{zz}^2 + 2\tau_{xy}^2 + 2\tau_{xz}^2 + 2\tau_{yz}^2\right) \\ J_3 = s_{xx} s_{yy} s_{zz} = 2\tau_{xy}\tau_{yz}\tau_{xz} - \sigma_{xx}\tau_{yz}^2 - \sigma_{yy}\tau_{xz}^2 - \sigma_{zz}\tau_{xy}^2 \end{cases} \tag{5}$$

~~It can be seen that the invariants of the deviatoric stress tensor J_1, J_2 and J_3 are related to the invariants of the stress tensor I_1, I_2 and I_3 through the following relations:~~

~~$$\begin{cases} J_1 = 0 \\ J_2 = \dfrac{1}{3}\left(I_1^2 - 3I_2\right) \\ J_3 = \dfrac{1}{27}\left(2I_1^3 - 9I_1 I_2 + 27I_3\right) \end{cases} \tag{7}$$~~

~~where t~~The deviatoric stress q can be calculated using the second invariant of the deviatoric stress tensor J_2.

$$q = \sqrt{3J_2} \tag{6}$$

In a triaxial test, the deviatoric stress q can be simplified to $q=|\sigma_a-\sigma_r|$, or $q=\sigma_a-\sigma_r$ to distinguish the compression or the extension conditions.

The lode angle θ can be calculated using the invariants of the deviatoric stress tensor as follows:

$$\cos 3\theta = \frac{3\sqrt{3}}{2} \frac{J_3}{J_2^{\frac{3}{2}}} \tag{7}$$

This works for a conventional triaxial compression test with $\sigma_2=\sigma_3$, b=0 and θ=0°; for a conventional triaxial extension test with $\sigma_2=\sigma_1$, b=1 and θ=60°; and when $\sigma_2=(\sigma_1+\sigma_3)/2$, b=0.5 and θ=30°. Note that b is the parameter of intermediate principal stress, and is defined as $b=(\sigma_2-\sigma_3)/(\sigma_1-\sigma_3)$).

The principal stress σ_1, σ_2 and σ_3 can be obtained as follows,

$$\begin{cases}\sigma_1=\dfrac{I_1}{3}+2\sqrt{\dfrac{J_2}{3}}\cos\theta\\ \sigma_2=\dfrac{I_1}{3}+\sqrt{\dfrac{J_2}{3}}\left(\cos\theta-\sqrt{3}\sin\theta\right)\\ \sigma_3=\dfrac{I_1}{3}+\sqrt{\dfrac{J_2}{3}}\left(\cos\theta+\sqrt{3}\sin\theta\right)\end{cases}\quad\text{or}\quad\begin{cases}\sigma_1=p+\dfrac{2}{3}q\cos\theta\\ \sigma_2=p+\dfrac{2}{3}q\cos\left(\theta-\dfrac{2\pi}{3}\right)\\ \sigma_3=p+\dfrac{2}{3}q\cos\left(\theta+\dfrac{2\pi}{3}\right)\end{cases}\tag{8}$$

2.2 Strain analysis

Under the small deformation condition, ~~the strain state at a point can be described by the strain tensor:~~

~~$$\varepsilon_{ij}=\begin{bmatrix}\varepsilon_x & \frac{1}{2}\gamma_{xy} & \frac{1}{2}\gamma_{xz}\\ \frac{1}{2}\gamma_{yx} & \varepsilon_y & \frac{1}{2}\gamma_{yz}\\ \frac{1}{2}\gamma_{zx} & \frac{1}{2}\gamma_{zy} & \varepsilon_z\end{bmatrix}\equiv\begin{bmatrix}\varepsilon_{xx} & \varepsilon_{xy} & \varepsilon_{xz}\\ \varepsilon_{yx} & \varepsilon_{yy} & \varepsilon_{yz}\\ \varepsilon_{zx} & \varepsilon_{zy} & \varepsilon_{zz}\end{bmatrix}\equiv\begin{bmatrix}\varepsilon_{11} & \varepsilon_{12} & \varepsilon_{13}\\ \varepsilon_{21} & \varepsilon_{22} & \varepsilon_{23}\\ \varepsilon_{31} & \varepsilon_{32} & \varepsilon_{33}\end{bmatrix}\tag{9}$$~~

~~where γ is the engineering shear strain.~~ the strain tensor can be divided into deviatoric and spherical tensors as follows:

$$\varepsilon_{ij}=\begin{bmatrix}\varepsilon_x-\varepsilon_m & \frac{1}{2}\gamma_{xy} & \frac{1}{2}\gamma_{xz}\\ \frac{1}{2}\gamma_{yx} & \varepsilon_y-\varepsilon_m & \frac{1}{2}\gamma_{yz}\\ \frac{1}{2}\gamma_{zx} & \frac{1}{2}\gamma_{zy} & \varepsilon_z-\varepsilon_m\end{bmatrix}+\begin{bmatrix}\varepsilon_m & 0 & 0\\ 0 & \varepsilon_m & 0\\ 0 & 0 & \varepsilon_m\end{bmatrix}=e_{ij}+\varepsilon_m\delta_{ij}\tag{9}$$

where γ is the engineering shear strain, e_{ij} is deviatoric strain tensor, and the mean strain ε_m is defined as $\varepsilon_m=\left(\varepsilon_x+\varepsilon_y+\varepsilon_z\right)/3$.

~~Similarly to the stress tensor, the invariants of the strain tensor are:~~

$$\begin{cases} I_1' = \varepsilon_x + \varepsilon_y + \varepsilon_z \\ I_2' = \varepsilon_x\varepsilon_y + \varepsilon_y\varepsilon_z + \varepsilon_z\varepsilon_x - \left(\frac{\gamma_{xy}}{2}\right)^2 - \left(\frac{\gamma_{yz}}{2}\right)^2 - \left(\frac{\gamma_{zx}}{2}\right)^2 \\ I_3' = \varepsilon_x\varepsilon_y\varepsilon_z + 2\left(\frac{\gamma_{xy}}{2}\right)\left(\frac{\gamma_{yz}}{2}\right)\left(\frac{\gamma_{zx}}{2}\right) - \varepsilon_x\left(\frac{\gamma_{yz}}{2}\right)^2 - \varepsilon_y\left(\frac{\gamma_{zx}}{2}\right)^2 - \varepsilon_z\left(\frac{\gamma_{xy}}{2}\right)^2 \end{cases} \quad (13)$$

The invariants of the deviatoric strain tensor are:

$$\begin{cases} J_1' = (\varepsilon_{xx} - \varepsilon_m) + (\varepsilon_{yy} - \varepsilon_m) + (\varepsilon_{zz} - \varepsilon_m) = 0 \\ J_2' = (\varepsilon_{xx} - \varepsilon_m)(\varepsilon_{yy} - \varepsilon_m) + (\varepsilon_{yy} - \varepsilon_m)(\varepsilon_{zz} - \varepsilon_m) + (\varepsilon_{zz} - \varepsilon_m)(\varepsilon_{xx} - \varepsilon_m) - \left(\frac{\gamma_{xy}}{2}\right)^2 - \left(\frac{\gamma_{yz}}{2}\right)^2 - \left(\frac{\gamma_{zx}}{2}\right)^2 \\ J_3' = (\varepsilon_{xx} - \varepsilon_m)(\varepsilon_{yy} - \varepsilon_m)(\varepsilon_{zz} - \varepsilon_m) + 2\left(\frac{\gamma_{xy}}{2}\right)\left(\frac{\gamma_{yz}}{2}\right)\left(\frac{\gamma_{zx}}{2}\right) - \varepsilon_x\left(\frac{\gamma_{yz}}{2}\right)^2 - \varepsilon_y\left(\frac{\gamma_{zx}}{2}\right)^2 - \varepsilon_z\left(\frac{\gamma_{xy}}{2}\right)^2 \end{cases} \quad (14)$$

The general shear strain ε_d is defined as:

$$\varepsilon_d = \sqrt{\frac{2}{3}e_{ij}e_{ji}} \quad \text{and} \quad \varepsilon_d = \frac{2}{3}(\varepsilon_1 - \varepsilon_3) \quad \text{for a triaxial test } (\varepsilon_2 = \varepsilon_3) \quad (10)$$

For a triaxial test ($\varepsilon_2 = \varepsilon_3$), the general shear strain ε_d can be reduced to:

The volumetric strain ε_v is (under the small deformation assumption):

$$\varepsilon_v = \frac{\Delta V}{V} = (1+\varepsilon_1)(1+\varepsilon_2)(1+\varepsilon_3) - 1 \approx \varepsilon_1 + \varepsilon_2 + \varepsilon_3 \quad (11)$$

3 ErosLab tool

3.1 Mixed-language programming

Fig. 1 shows the schematic overview of the mixed-language programming for ErosLab. The tool is programmed using the admixture method, with Microsoft Visual C#, MATLAB and FORTRAN. The graphical user interface is programmed in C#, the post-processing (for plotting the figure, exporting the results, generating the report and reading the help documentation) is realised using MATLAB, and the constitutive models are programmed in FORTRAN. All MATLAB files are built as dynamic library files (*.dll) under the .NET Framework 4.0. The version of MATLAB used is MATLAB 2016b.

3.2 General structure of ErosLab

The general structure of ErosLab is shown in Fig. 2 and the six main features are summarised in this section.

3.2.1 Provision of a mechanical calculator

The tool provides a practical mechanical calculator. For a given stress tensor σ_{ij}, the invariants of the stress tensor (I_1, I_2 and I_3), the invariants of the deviatoric stress tensor (J_1, J_2 and J_3), the principal stress (σ_1, σ_2 and σ_3), the mean stress p, the deviatoric stress tensor s_{ij}, the deviatoric stress q, the lode angle θ, and the directions of principal stresses (l, m and n) can be obtained. Furthermore, the transformation of coordinates can also be achieved. For a given strain tensor, the invariants of the strain tensor (I'_1, I'_2 and I'_3), the invariants of the deviatoric strain tensor (J'_1, J'_2 and J'_3), the principal strain (ε_1, ε_2 and ε_3), the mean strain ε_m, the deviatoric stress tensor e_{ij}, and the deviatoric strain ε_d, can be similarly obtained. The stress and strain analysis can be conducted rapidly via the mechanical calculator provided by ErosLab, which is useful for study and research purposes.

3.2.2 Provision of various types of soil tests

A range of common laboratory tests are provided in this tool, including the oedometer test, the triaxial test, the simple shear test, the biaxial test, true triaxial test, and the cylindrical hollow torsional shear test. Compared to PLAXIS, the proposed tool offers a greater variety of types of laboratory tests. The laboratory tests available in ErosLab are briefly introduced below.

In the tool, the oedometer test is simulated as a one-dimensional compression test, where the lateral deformation is constrained to zero and only vertical deformation is allowed. The lateral stress necessarily keeps changing during the loading process because of the restriction of lateral deformation. Therefore, the test can be conveniently controlled by pure strain loading or strain-and-stress mixed loading. Note that the proposed ErosLab has difficulty in conducting the conventional 24h oedometer test because of lacking implementation of soil-water coupling analysis, which will be available in further development for finite element analysis tool.

For the conventional consolidated drained triaxial compression test, the soil sample is first consolidated to a given confining pressure; then, the axial load is increased up to the failure of the sample while keeping the confining pressure constant. The slope of this loading path in the p'-q plane is 3. For the conventional consolidated undrained triaxial compression test, the increment of total confining stress is kept constant; thus, the slope of the loading path on the p-q plane remains 3.Under the conventional confining pressure, both the soil particle and the water are considered incompressible, creating the possibility of fulfilling the undrained condition by keeping the volumetric strain constant. In this way, whether compression or extension occurs depends on the increasing or decreasing of the axial strain respectively. In this program, all undrained simulations (except for the creep simulation using the ANICREEP model) are performed by keeping the volumetric strain constant.

In the simple shear test, the shear strain (γ) is defined as the ratio of the horizontal displacement to the sample height. Under the loading of vertical shear strain, the shear stress, vertical stress and vertical displacement can be obtained using a simple shear test. Two options exist for conducting this simple shear test: (1) keeping a constant vertical load, which is the drained simple shear test, and (2) keeping the volume of the sample constant, which can be regarded as the undrained simple shear test.

The aim of the biaxial test is to study the stress-strain-strength behaviours of soil in a plane-strain condition. For this test, the displacement in the perpendicular to the plane is constrained to zero and the lateral of the sample is constrained by applying a horizontal confining pressure (σ_h). Then, the sample is loaded by applying a vertical load (either by displacement ε_v or stress σ_v).

The purpose of the true triaxial apparatus is to study the stress-strain-strength behaviours of soil in a 3D condition. Since all 3D stresses can be controlled respectively, the true triaxial test can make many complicated stress paths a reality. A common stress path is to carry out a series of drained shear tests with different constant intermediate principal stress factors b (b=(σ_2-σ_3)/ (σ_1-σ_3)), or lode angle (θ), while keeping the mean stress constant. p' and b, as input values are known; that is, the

sample is loaded to failure by increasing the major principal stress along with the intermediate and minor principal stress calculated according to Eq.(12).

$$\begin{cases} p' = \dfrac{\sigma_1' + \sigma_2' + \sigma_3'}{3} \\ b = \dfrac{\sigma_2' - \sigma_3'}{\sigma_1' - \sigma_3'} \end{cases} \Rightarrow \begin{cases} \sigma_2' = \dfrac{3(1-b)p' + (2b-1)\sigma_1'}{2-b} \\ \sigma_3' = \dfrac{3p' - (1+b)\sigma_1'}{2-b} \end{cases} \Rightarrow \begin{cases} d\sigma_2' = \dfrac{(2b-1)}{2-b} d\sigma_1' \\ d\sigma_3' = \dfrac{-(1+b)}{2-b} d\sigma_1' \end{cases} \tag{12}$$

The hollow cylinder torsional shear test is an effective means of studying the influence of principal stress rotation on the stress-strain relationship and the anisotropy of soil. When the principal stress does not rotate, the apparatus can also be used to conduct the true triaxial test in different stress paths. In the program, the sample is first isotropically compressed to a confining pressure, then kept constant; loading is applied by changing the values of q, α and b, as shown in Eq.(13).

$$\begin{cases} \sigma_1 = p + \dfrac{2-b}{3\sqrt{b^2-b+1}} q \\ \sigma_2 = p + \dfrac{2b-1}{3\sqrt{b^2-b+1}} q + \\ \sigma_3 = p - \dfrac{b+1}{3\sqrt{b^2-b+1}} q \end{cases} \begin{cases} \sigma_z = \dfrac{\sigma_1+\sigma_3}{2} + \dfrac{\sigma_1-\sigma_3}{2}\cos(2\alpha) \\ \sigma_r = \sigma_2' \\ \sigma_\theta = \dfrac{\sigma_1+\sigma_3}{2} - \dfrac{\sigma_1-\sigma_3}{2}\cos(2\alpha) \\ \tau_{z\theta} = \dfrac{\sigma_1-\sigma_3}{2}\sin(2\alpha) \end{cases} \Rightarrow \begin{cases} \sigma_z = p' + \dfrac{1-2b}{6\sqrt{b^2-b+1}} q + \dfrac{1}{2\sqrt{b^2-b+1}} q\cos(2\alpha) \\ \sigma_r = p' + \dfrac{2b-1}{3\sqrt{b^2-b+1}} q \\ \sigma_\theta = p' + \dfrac{1-2b}{6\sqrt{b^2-b+1}} q - \dfrac{1}{2\sqrt{b^2-b+1}} q\cos(2\alpha) \\ \tau_{z\theta} = \dfrac{1}{2\sqrt{b^2-b+1}} q\sin(2\alpha) \end{cases} \tag{13}$$

3.2.3 Provision of a variety of soil models and supporting of the extension

In ErosLab, a total of six soil constitutive models (Perfect EP, NLMC, MCC, SIMSAND, ASCM and ANICREEP) are provided, which covers most commonly adopted mechanical soil models. Other advanced soil models will be available in the next version of ErosLab. There follows short descriptions of the presented soil models.

The perfect elastoplastic model (Perfect EP) is a series of perfect elastoplastic models involving different yield criteria (the Von-Mises, Tresca, Mohr-Coulomb, SMP and g(θ) of Sheng). The Nonlinear Mohr-Coulomb model (NLMC) was developed against the framework of Mohr-Coulomb, by implementing nonlinear elasticity, nonlinear plastic hardening, and a simplified 3D strength

criterion (Jin et al., 2016a)[30]. The model is similar to the shearing element of the Hardening Soil model (HS). The Modified Cam-Clay model (MCC) was developed by researchers at the University of Cambridge, based on the mechanical behaviour of remoulded clay (Roscoe & Burland[31]) and is widely used for geotechnical analysis. The critical-state-based SIMple SAND model (SIMSAND) was developed on the basis of the NLMC by implementing the critical state concept and the capping mechanism (Jin et al., 2016a, 2016b) [30, 32]. The Anisotropic Structured Clay Model (ASCM) was developed with the MCC as its foundation and takes into account the behaviour of intact clays because of its natural structure (Yang et al.[33]). The model can be used to predict the mechanical behaviour of soft structured clay, stiff clay and artificially reinforced clay. The ANIsotropic CREEP model (ANICREEP), for natural soft clays, was also based on the MCC, as well as the overstress theory and the different time-dependent behaviours of such clays (Yin et al. [5, 34, 35]). The ANICREEP can be applied to a range of natural soft clays, stiff clays and artificial soils.

To improve the extensibility of the proposed tool, the user-defined material (UMAT) is supported, which allows the user to implement other soil models in ErosLab Fig. 3 shows an interface module of UMAT written in the FORTRAN language. A **.dll* file can be compiled by adopting the Intel FORTRAN 32 bit as the compiler tool. Thereafter, the **.dll* file should be renamed "Umat.dll" and placed into the same directory as the main program of ErosLab. Then, the user-defined material can be found in the tool. Note that the name of the subroutine must be "Umat" (altering this will lead to errors). IDtask is the task number. IDtask=1 is the initialisation of the state variables; IDtask=2 calculates the elastic matrix; and IDtask=3 updates the stress and state variables. The cm is a vector with the material parameters; deps is the strain increment; sig is the stress; hsv is the state variables; and CC is the elastic matrix tensor. Other parameters and state variables can be defined by the user. "!DEC$ ATTRIBUTES DLLEXPORT, DECORATE, ALIAS: 'Umat' :: Umat" is the statement of the subroutine name.

3.2.4 Provision of multiple ways of loading control

Two conventional loading methods are provided: (a) monotonic loading and (b) cyclic loading. For the former, the loading of stress control and strain control for all laboratory tests is available. To

efficiently conduct the simulation, one-stage and multi-stage loading can be alternatively chosen by the user; for example, the arbitrary stress or strain path can be simulated for the triaxial test. For cyclic loading, the cyclic stress control and strain control are allowed. Note that the function takes effect only when the selected constitutive model is able to reproduce the cyclic behaviours of soil. Diversified loading control provides greater possibilities for users to deeply and comprehensively understand the constitutive model.

3.2.5 Provision of a comprehensive and efficient debugging

It is important to debug a newly developed constitutive model before applying it to solve engineering problems. ErosLab offers a comprehensive and efficient debugging for four kinds of laboratory tests (the oedometer tests, the triaxial test, the simple shear test and the true triaxial test). When debugging is invoked, potential issues with a soil model can be discovered by using it to successively simulate the four types of test along different stress paths. This function can give a new model greater robustness in the numerical calculation. Note that the debugging is in an elementary stage with complex loading combinations which reflects somehow the in-situ conditions. Therefore, even though no simulation of in-situ problems can be directly conducted, the current debugging scheme for a newly developed model should be effective for the practical purpose. ~~and thus f~~Further possible problems can be investigated by implementing the model in the numerical software.

3.2.6 Provision of visualisation with graphical displays

The graphic user interface (GUI) of the developed software is composed of seven interface objects: Main Form, Test-type Form, Constitutive Model Form, Drainage Condition Form, Loading Condition Form, Data Management Form and Command Form. The Main Form interacts with the user and connects to the other forms, the functionalities of which can be recognised from their names. The Test-type Form defines the type of laboratory tests provided and the initial stress state. The Constitutive Model Form allows the user to select the constitutive model and set the parameters. The Drainage Condition Form provides a selection of drainage conditions for the chosen laboratory test. The Loading Condition Form offers a variety of loading controls for different tests. The Data

Management Form enables the importing of experiments, exporting of the simulated data and generating reports. The Command Form is used to give the commands to run, stop and exit the program.

4 Graphical user interface and usage instructions

4.1 Graphical user interface

Fig. 4 shows ErosLab's main interface, which is divided into six zones: *Test type*, *Constitutive model*, *Drainage condition*, *Loading condition*, *Data management* and *Command*. For the *Test type* and *Constitutive model*, a graphic illustration showing the user's choice is provided. The forms for stress and strain and the debug are presented separately.

Fig. 5 shows the GUI window for selecting the test and setting the initial stress. All the tests provided are important for highlighting the behaviours of a constitutive model. After selection, the initial stress corresponding to the general stress state should be given. Note that the initial suction only works for the constitutive model of unsaturated soils; this will be addressed in the next version.

To allow the user greater choice, a variety of constitutive models accounting for different mechanical behaviours are collected and implemented into the ErosLab tool. Fig. 6 (a) shows the GUI window for selecting the soil model. Note that some constitutive models are temporarily not available in current platform, which are marked as grey items. More useful constitutive models will be included in the next version of ErosLab. After selecting the soil model, the corresponding parameters should be given, as shown in Fig. 6 (b), which takes the SIMSAND as an example. Fig. 7, meanwhile, shows the GUI window of parameter input for UMAT. In current version, any constitutive model can be used only if the name of subroutine is signed as UMAT. A total of ~~20~~ 30 parameters are defined for the UMAT, which is enough for most existing constitutive models and even for newly developed examples. It should be pointed out that the determination of model parameters is an important work, which arises the challenge with increasing the number of parameters, especially for advanced soil models. To author's knowledge, the newly developed

optimization-based parameter identification [30, 36-41] would be useful and can be incorporated into the proposed tool in next version.

To show the user how to select an appropriate constitutive model for his test, a user's manual explaining the capabilities and applicability of each constitutive model is provided, illustrated with tutorial examples, which can be downloaded from the website: http://www.geoinvention.com/en/newsshow.asp?id=244&big=14.

Fig. 8 displays the GUI window of monotonic loading for the triaxial test. For said test, a consolidation stage prior to the shearing can be selected by giving a confining stress. Otherwise, the values of said stress are kept the same as those of the initial stress. The displayed σ_a is the axial confining stress, and σ_r is the radial confining stress. $\sigma_r=\sigma_a$ refers to the isotropic consolidation and $\sigma_r\neq\sigma_a$ refers to the anisotropic consolidation. The loading time only works for the models that account for the time-dependent behaviours of soil (ANICREEP in this version). Two loading methods of shearing are provided. Apart from the conventional triaxial tests, the creep and relaxation triaxial tests can be easily and adequately simulated by the ErosLab tool, which is superior to other tools for modelling soil tests. Moreover, the simulation of any stress or strain path can be achieved by multi-stage loading, the GUI window for which is shown in Fig. 9. In total, six stages are allowed, and more may be added in the future. The functionality of multi-stage loading control is powerful, a quality that cannot be found in other similar tools. Because of the length of this paper, the GUI windows of other tests are not presented here, but can be found in the ErosLab tool.

In addition to the abovementioned GUI windows, those for stress and strain analysis and for debugging remain to be illustrated. Fig. 10 exhibits the GUI window for the stress and strain analysis; most stress- or strain-related variables can be obtained via this window. Fig. 11 displays the GUI window for debugging, which specifies the setups of loading for different tests. For the triaxial test in debugging, three tests with loading, unloading and reloading under different confining pressures will be simulated and presented. Similarly, the oedometer and simple shear tests are the same situations compared to the triaxial test. For the true triaxial test, a yield surface in π plane for the selected

constitutive model can be obtained from the simulations with different values of *b* from 0 to 1 in a step size of 0.1.

4.2 Usage instructions

The basic procedure for using the ErosLab tool to simulate a laboratory test can be divided into six steps:

Step 1: Select the test type and set the initial stress.

Step 2: Select the soil model and assign the model parameters.

Step 3: Select the drainage condition.

Step 4: Set the loading condition.

Step 5: Run the tool.

Step 6: Export the simulated results.

Step 7: Generate the report.

5 Case studies

In this section, the results of three case studies are described that were conducted to showcase the performance of ErosLab. To cover most kinds of soils, the first case is the use of SIMSAND to simulate the sand behaviour (e.g., dilatancy, contractiveness, static and cyclic liquefactions); the second case is the use of ASCM to model the behaviour of natural clays (e.g., structure, anisotropy and cyclic densification); the last case is the use of ANICREEP to model the time-dependent behaviour of soft clays.

5.1 Case 1: Modelling of sand behaviours by SIMSAND

The tests selected for this case were triaxial tests performed on Hostun sand by Liu et al. [42] and Li et al. [43]. All the tests were isotropically consolidated to the corresponding consolidation pressure before shearing. Fig. 12 shows the adopted parameters of SIMSAND for simulating the behaviour of Hostun sand, where the line represents the simulations and the red circle points represent the experimental results. All parameters refer to the results of Jin et al. [30, 44].

First, three drained triaxial tests with different confining pressures and initial void ratios on Hostun sand were simulated using the SIMSAND model via the proposed tool. Then, four undrained triaxial tests with different confining pressures and initial void ratios on said sand were also simulated in a similar way. Fig. 13 (a) shows the comparisons between the simulations and experiments for the drained tests, while Fig. 13 (b) does the same for the undrained tests. It can be seen that the proposed tool offers many ways of displaying simulated results (ε_a -q, p'-q, time- ε_a, e-ε_a, e-p', and time-p', q), which provides a comprehensive method of understanding a constitutive model. Moreover, all the comparisons, with good agreement, demonstrate that the sand behaviours (such as contraction, dilation, the critical state and interlocking effect) can be adequately reproduced via SIMSAND in ErosLab.

To show ErosLab's ability on the loading control, the cyclic test was simulated using SIMSAND for sand. The same parameters, corresponding to Hostun sand, were used. In this case, a two-way cyclic test with a value of cyclic stress 20 kPa was selected and simulated. Because experiments were not available, only the simulated results are presented. Fig. 14 (a) and (b) show the simulations of drained and undrained cyclic triaxial tests using SIMSAND, respectively, while Fig. 14 (c) shows the simulations of the undrained cyclic simple shear test using the same model. It may be observed that the modelling of cyclic tests can be adequately achieved using the ErosLab tool. Furthermore, the results also indicate that the SIMSAND model has an outstanding ability to reproduce the cyclic behaviours of sand (for example, its densification in drained conditions and mobilisation in undrained conditions).

5.2 Case 2: Modelling of clay behaviours using ASCM

In this case, four undrained triaxial tests performed on Shanghai clay were simulated via the ErosLab tool using the ASCM model. According to Huang *et al.* [45], undisturbed samples of Shanghai clay were taken at depths of 10 m, with in-situ horizontal consolidation stress σ'_{hc}= 41 kPa and vertical consolidation stress σ'_{vc}= 68.6 kPa. The initial mean effective stress p'_c was determined as 50.3 kPa. The parameters of ASCM employed for Shanghai clay are shown in Fig. 15, these were collected from results garnered by Yang et al. [33] and Ye et al. [46].

First, two isotropically-consolidated undrained compression tests (CIUC) were simulated. The simulations were compared to the experiments, as shown in Fig. 16 (a). Similarly, another two anisotropically consolidated undrained compression tests (CAUC) were then simulated. The comparisons between the simulations and experiments are shown in Fig. 16 (b). Furthermore, the cyclic behaviours can also be captured by using ASCM via ErosLab. Fig. 17 (a) and (b) display the simulations of drained and undrained cyclic tests by ASCM, respectively.

The results denote that the provided ASCM model can reproduce the anisotropy and destructuration behaviours for normal and over-consolidated natural clays undergoing monotonic and cyclic loadings.

5.3 Case 3: Modelling of time effects of clay behaviours by ANICREEP

A series of undrained triaxial tests in both compression and extension conditions at three different strain rates (0.2 %/h, 2 %/h and 20 %/h) on K_0-consolidated Wenzhou clay were selected and simulated using the ANICREEP model in the ErosLab tool. The Wenzhou clay deposit is a marine clay characterised as slightly organic and highly plastic. Intensive laboratory tests were conducted out along various stress paths, focusing on the rate-dependent mechanical properties of Wenzhou clay (Yin et al. [35]). The parameters of ANICREEP for Wenzhou clay were obtained from the study by Yin et al. [47]. Fig. 18 shows the employed parameters of ANICREEP that correspond to Wenzhou clay in ErosLab.

Three sets of undrained triaxial tests in compression and extension under vertical effective stress (σ'_{v0}= 150 kPa) at strain-rates of 0.2 %/h, 2 %/h and 20 %/h were simulated. Fig. 19 (a) and (b) show the comparisons between the simulated and measured results of three different strain-rates, respectively. Good agreement between the experimental results and simulations was generally achieved using the ANICREEP model. The results demonstrate that the behaviours of strain rate dependency, combined with anisotropy and the destructuration of natural soft clays, can be adequately captured by the ANICREEP model.

6 Conclusions

In this paper, the development of ErosLab, a modelling tool for soil tests, was described. ErosLab also offers support for both research and teaching as regards the practice of constitutive models in the fields of geomechanics and geotechnics. Simple and clear interfaces render the tool easily used by engineers; for example, the friendly graphical interface can help users view and analyse results. Various constitutive models can be used with an open interface for the user-defined model. The performance of different models can be compared and their results discussed. Three selected case studies to simulate the behaviours of sand and clays were carried out, the results proving that ErosLab is a useful tool in engineering practice.

Furthermore, this study can be used for the teaching purpose to present the basic constitutive modelling of soil behaviours for postgraduate students who major on civil engineering, water conservancy, transportation, railway and engineering geology. It also can be used for the purpose of the relevant professional scientific research.

In future work, the tool can be extended by using other advanced constitutive models for more types of tests. With the growing ubiquity of the Internet, a discussion window will be added for easy online communication and exchange, which will foster the growth of an ErosLab community.

Acknowledgments

The financial support for this research came from the National Natural Science Foundation of China (41372285, 51579179), and the Region Pays de la Loire of France (project RI-ADAPTCLIM)

References

[1] Li Z, Kotronis P, Escoffier S, Tamagnini C. A hypoplastic macroelement for single vertical piles in sand subject to three-dimensional loading conditions. Acta Geotech 2016;11:373-90.

[2] Yin ZY, Chang CS, Hicher PY. Micromechanical modelling for effect of inherent anisotropy on cyclic behaviour of sand. Int J Solids Struct 2010;47:1933-51.

[3] Yin ZY, Chang CS, Hicher PY, Karstunen M. Micromechanical analysis of kinematic hardening in natural clay. Int J Plast 2009;25:1413-35.

[4] Yu M-h. Advances in strength theories for materials under complex stress state in the 20th century. Appl Mech Rev 2002;55:169-218.

[5] Yin ZY, Chang CS, Karstunen M, Hicher PY. An anisotropic elastic-viscoplastic model for soft clays. Int J Solids Struct 2010;47:665-77.

[6] Yao Y, Hou W, Zhou A. UH model: three-dimensional unified hardening model for overconsolidated clays. Geotechnique. 2009;59:451-69.

[7] Yao Y, Sun D, Matsuoka H. A unified constitutive model for both clay and sand with hardening parameter independent on stress path. Computers and Geotechnics. 2008;35:210-22.

[8] Yao Y-P, Kong L-M, Zhou A-N, Yin J-H. Time-dependent unified hardening model: Three-dimensional elastoviscoplastic constitutive model for clays. Journal of engineering mechanics. 2014;141:04014162.

[9] Yao Y-P, Yamamoto H, Wang N-D. Constitutive model considering sand crushing. Soils and Foundations. 2008;48:603-8.

[10] Jin Y-F, Yin Z-Y, Wu Z-X, Daouadji A. Numerical modeling of pile penetration in silica sands considering the effect of grain breakage. Finite Elem Anal Des 2018;144:15-29.

[11] Potts D. Numerical analysis: a virtual dream or practical reality? Géotechnique. 2003;53:535-73.

[12] Lim A, Ou C-Y, Hsieh P-G. Evaluation of clay constitutive models for analysis of deep excavation under undrained conditions. Journal of Geoengineering. 2010;5:9-20.

[13] Karstunen M, Yin ZY. Modelling time-dependent behaviour of Murro test embankment. Geotechnique. 2010;60:735-49.

[14] Yin Z, Karstunen M, Wang J, Yu C. Influence of features of natural soft clay on behaviour of embankment. Journal of Central South University of Technology. 2011;18:1667-76.

[15] Wu H-N, Shen S-L, Ma L, Yin Z-Y, Horpibulsuk S. Evaluation of the strength increase of marine clay under staged embankment loading: a case study. Marine Georesources & Geotechnology. 2015;33:532-41.

[16] Zhang N, Shen S-L, Wu H-N, Chai J-C, Xu Y-S, Yin Z-Y. Evaluation of effect of basal geotextile reinforcement under embankment loading on soft marine deposits. Geotext Geomembr 2015;43:506-14.

[17] Whittle A, Davies R. Nicoll Highway collapse: evaluation of geotechnical factors affecting design of excavation support system. International conference on deep excavations2006. p. 30.

[18] Chai J, Shen S, Ding W, Zhu H, Carter J. Numerical investigation of the failure of a building in Shanghai, China. Computers and Geotechnics. 2014;55:482-93.

[19] Shen S-L, Cui Q-L, Ho C-E, Xu Y-S. Ground response to multiple parallel microtunneling operations in cemented silty clay and sand. Journal of Geotechnical and Geoenvironmental Engineering. 2016;142:04016001.

[20] Shen S-L, Wu H-N, Cui Y-J, Yin Z-Y. Long-term settlement behaviour of metro tunnels in the soft deposits of Shanghai. Tunnelling and Underground Space Technology. 2014;40:309-23.

[21] Wu H-N, Shen S-L, Liao S-M, Yin Z-Y. Longitudinal structural modelling of shield tunnels considering shearing dislocation between segmental rings. Tunnelling and Underground Space Technology. 2015;50:317-23.

[22] Hibbitt, Karlsson, Sorensen. ABAQUS/Explicit: User's Manual: Hibbitt, Karlsson and Sorenson; 2001.

[23] Itasca F. Fast Lagrangian analysis of continua. Itasca Consulting Group Inc, Minneapolis, Minn. 2000.

[24] Brinkgreve R, Engin E, Swolfs W. Plaxis 2D 2012 user manual. Delft, Netherlands: Plaxis bv. 2012.

[25] Comsol A. COMSOL multiphysics user's guide. Version: September. 2005;10:333.

[26] Novák D, Vořechovský M, Teplý B. FReET: Software for the statistical and reliability analysis of engineering problems and FReET-D: Degradation module. Advances in Engineering Software. 2014;72:179-92.

[27] Wang H, Li L, Jiao Y-Y, Ge X-R, Li S-C. A relationship-based and object-oriented software for monitoring management during geotechnical excavation. Advances in Engineering Software. 2014;71:34-45.

[28] Yang Z, Lu J, Elgamal A. A web-based platform for computer simulation of seismic ground response. Advances in Engineering Software. 2004;35:249-59.

[29] Langtangen HP. A FEniCS tutorial. Automated Solution of Differential Equations by the Finite Element Method: Springer; 2012. p. 1-73.

[30] Jin Y-F, Yin Z-Y, Shen S-L, Hicher P-Y. Selection of sand models and identification of parameters using an enhanced genetic algorithm. Int J Numer Anal Methods Geomech 2016;40:1219-40.

[31] Roscoe KH, Burland J. On the generalized stress-strain behaviour of wet clay. Engineering Plasticity Cambridge, UK: Cambridge University Press; 1968. p. 535-609.

[32] Jin Y-F, Yin Z-Y, Shen S-L, Hicher P-Y. Investigation into MOGA for identifying parameters of a critical-state-based sand model and parameters correlation by factor analysis. Acta Geotech 2016;11:1131-45.

[33] Yang J, Yin Z-Y, Huang H-W, Jin Y-F, Zhang D-M. A bounding surface plasticity model of structured clays using disturbed state concept based hardening variables. Chinese Journal of Geotechnical Engineering. 2017;39:554-61.

[34] Yin ZY, Karstunen M, Chang CS, Koskinen M, Lojander M. Modeling Time-Dependent Behavior of Soft Sensitive Clay. Journal of geotechnical and geoenvironmental engineering. 2011;137:1103-13.

[35] Yin Z-Y, Yin J-H, Huang H-W. Rate-Dependent and Long-Term Yield Stress and Strength of Soft Wenzhou Marine Clay: Experiments and Modeling. Marine Georesources & Geotechnology. 2015;33:79-91.

[36] Jin Y-F, Wu Z-X, Yin Z-Y, Shen JS. Estimation of critical state-related formula in advanced constitutive modeling of granular material. Acta Geotech 2017;12:1329-51.

[37] Jin Y-F, Yin Z-Y, Shen S-L, Zhang D-M. A new hybrid real-coded genetic algorithm and its application to parameters identification of soils. Inverse Problems in Science and Engineering. 2017;25:1343-66.

[38] Jin Y-F, Yin Z-Y, Wu Z-X, Zhou W-H. Identifying parameters of easily crushable sand and application to offshore pile driving. Ocean Eng 2018;154:416-29.

[39] Wu Z-X, Yin Z-Y, Jin Y-F, Geng X-Y. A straightforward procedure of parameters determination for sand: a bridge from critical state based constitutive modelling to finite element analysis. European Journal of Environmental and Civil Engineering. 2017:1-23.

[40] Yin Z-Y, Jin Y-F, Shen JS, Hicher P-Y. Optimization techniques for identifying soil parameters in geotechnical engineering: Comparative study and enhancement. Int J Numer Anal Methods Geomech 2018;42:70-94.

[41] Yin Z-Y, Jin Y-F, Shen S-L, Huang H-W. An efficient optimization method for identifying parameters of soft structured clay by an enhanced genetic algorithm and elastic–viscoplastic model. Acta Geotech 2017;12:849-67.

[42] Liu Y-J, Li G, Yin Z-Y, Dano C, Hicher P-Y, Xia X-H, et al. Influence of grading on the undrained behavior of granular materials. CR Mec 2014;342:85-95.

[43] Li G, Liu Y-J, Dano C, Hicher P-Y. Grading-Dependent Behavior of Granular Materials: From Discrete to Continuous Modeling. Journal of engineering mechanics. 2014; 141(6), 04014172.

[44] Jin Y-F, Wu Z-X, Yin Z-Y, Shen JS. Estimation of critical state-related formula in advanced constitutive modeling of granular material. Acta Geotech 2017; 12(6), 1329-1351.

[45] Huang M, Liu Y, Sheng D. Simulation of yielding and stress–stain behavior of shanghai soft clay. Computers and Geotechnics. 2011;38:341-53.

[46] Ye L, Jin Y-F, Shen S-L, Sun P-P, Zhou C. An efficient parameter identification procedure for soft sensitive clays. Journal of Zhejiang University SCIENCE A. 2016;17:76-88.

[47] Yin Z-Y, Jin Y-F, Shen S-L, Huang H-W. An efficient optimization method for identifying parameters of soft structured clay by an enhanced genetic algorithm and elastic–viscoplastic model. Acta Geotech 2016:1-19.

Figure captions

~~Fig. 25 Comparisons between simulated and experimental results of undrained triaxial extension CRS tests at a vertical stress of 150 kPa~~

Figure 1

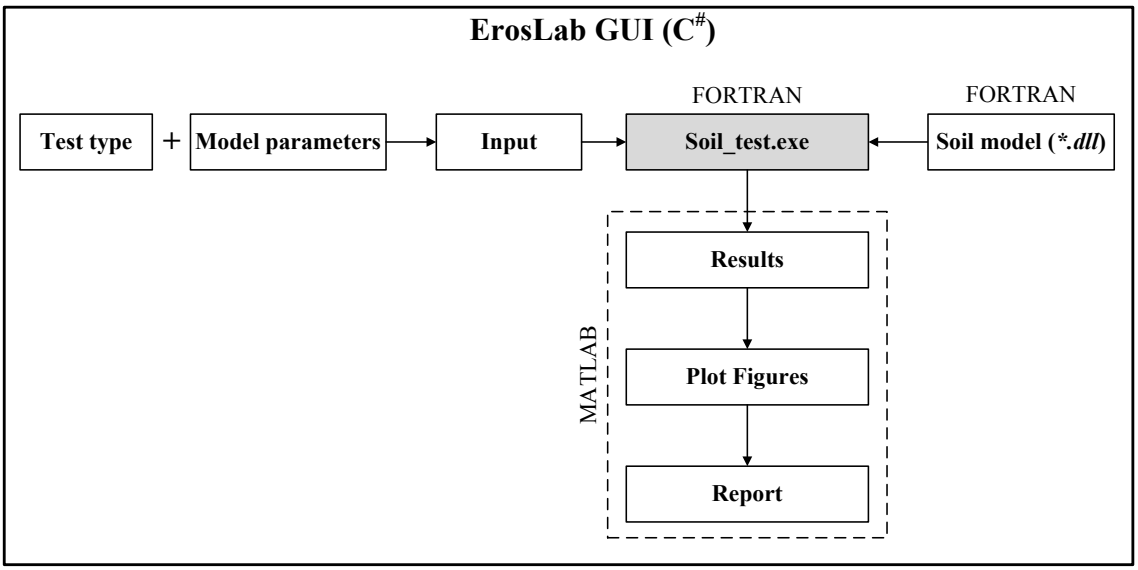
ErosLab GUI (C#)
FORTRAN
FORTRAN
Test type
+
Model parameters
Input
Soil_test.exe
Soil model (*.dll)
Results
Plot Figures
Report
MATLAB

Figure 2

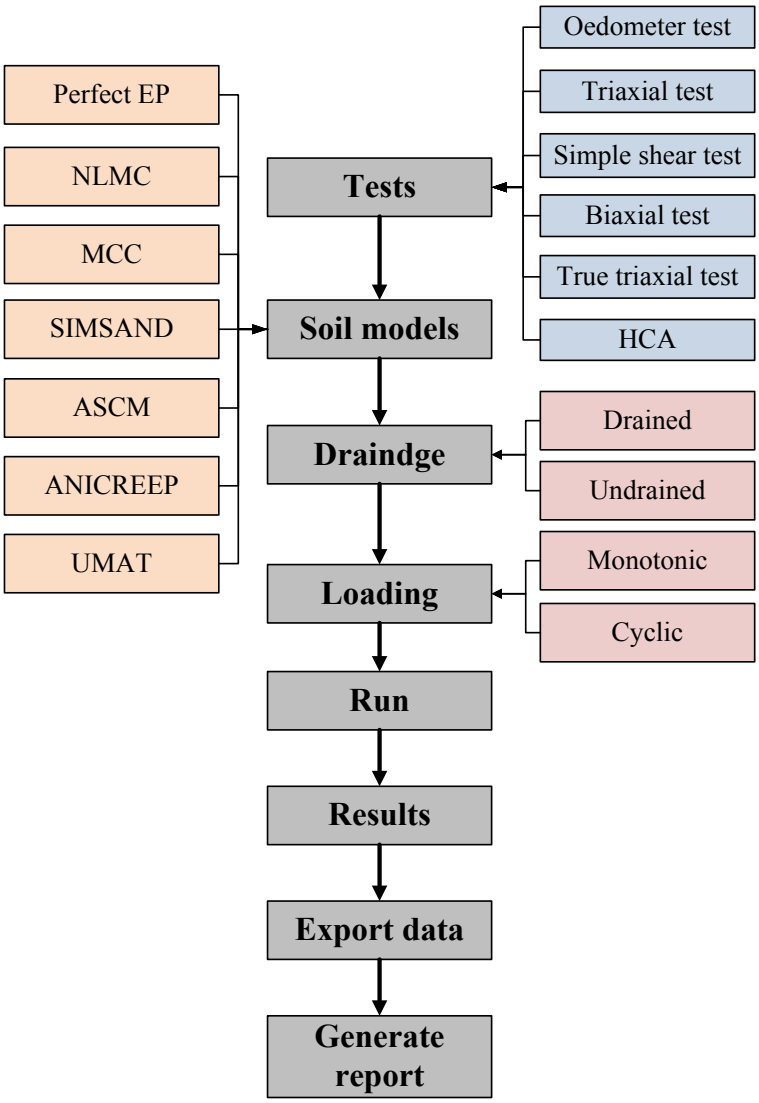
Perfect EP
NLMC
MCC
SIMSAND
ASCM
ANICREEP
UMAT
Tests
Soil models
Draindge
Loading
Run
Results
Export data
Generate report
Oedometer test
Triaxial test
Simple shear test
Biaxial test
True triaxial test
HCA
Drained
Undrained
Monotonic
Cyclic

Figure 3

```
!-----------------------------------------------------------------------
    Subroutine Umat (IDtask,cm,deps,sig,hsv,CC,dTime)

      !DEC$ ATTRIBUTES DLLEXPORT, DECORATE, ALIAS:"Umat" :: Umat

      Implicit Double Precision (A-H, O-Z)
      Double Precision cm(50),hsv(50),deps(6),deps0(6),epsp(6)
      Double Precision Sig(6),CC(6,6),Adding the defitions...
      Integer   etype, IDtask
      Logical     ::    converged       ! convergence for iteration

!---------------------------------------
      ! parameters definition
        xNu     = cm(1)  ! Poisson's ratio
        dkappa  = cm(2)  ! Swelling index
        dlambda = cm(3)  ! Compression index
        ......Please add parameters the user needs
!---------------------------------------    -------------------------
      if (IDtask.eq. 1) then
        hsv = 0.
        hsv(1)=e0        ! size of yield surface
        hsv(2)=0.        ! PORE pressure
        hsv(3)=pm0       ! void ratio
        ......Please add state variables the user needs
      end if
!---------------------------------------    -------------------------
      if (IDtask.eq. 2) then

        call MATRIXDE (Sig,cm,hsv,CC)  !Elastic stiffness matrix

      end if
!-----------------------------------------
      if (IDtask.eq. 3) then

        ......Please update stress and state variables

       end if

    Return

    end Subroutine
```

Figure 4

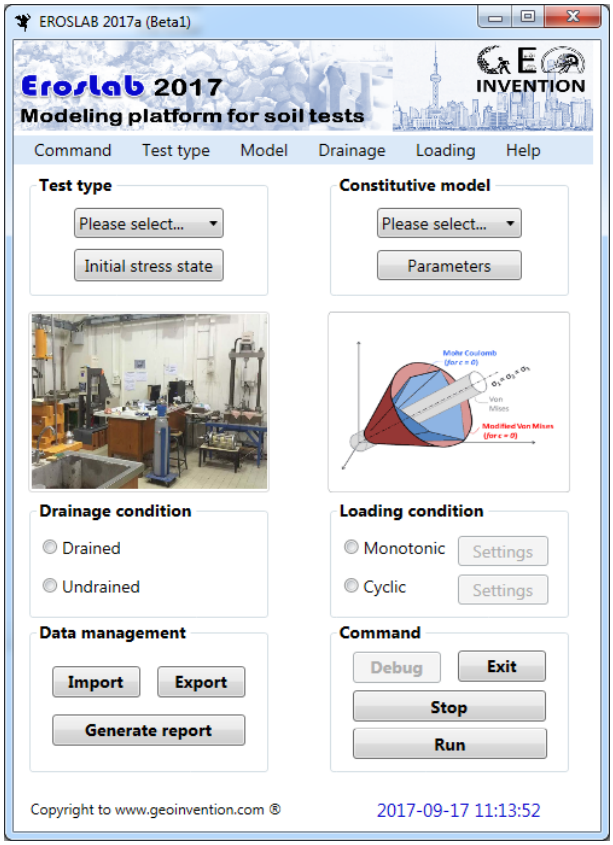
EROSLAB 2017a (Beta1)
Eroslab 2017
Modeling platform for soil tests
GEO INVENTION
Command
Test type
Model
Drainage
Loading
Help
Test type
Please select...
Initial stress state
Constitutive model
Please select...
Parameters
Drainage condition
Drained
Undrained
Loading condition
Monotonic
Settings
Cyclic
Settings
Data management
Import
Export
Generate report
Command
Debug
Exit
Stop
Run
Copyright to www.geoinvention.com ®
2017-09-17 11:13:52

Figure 5

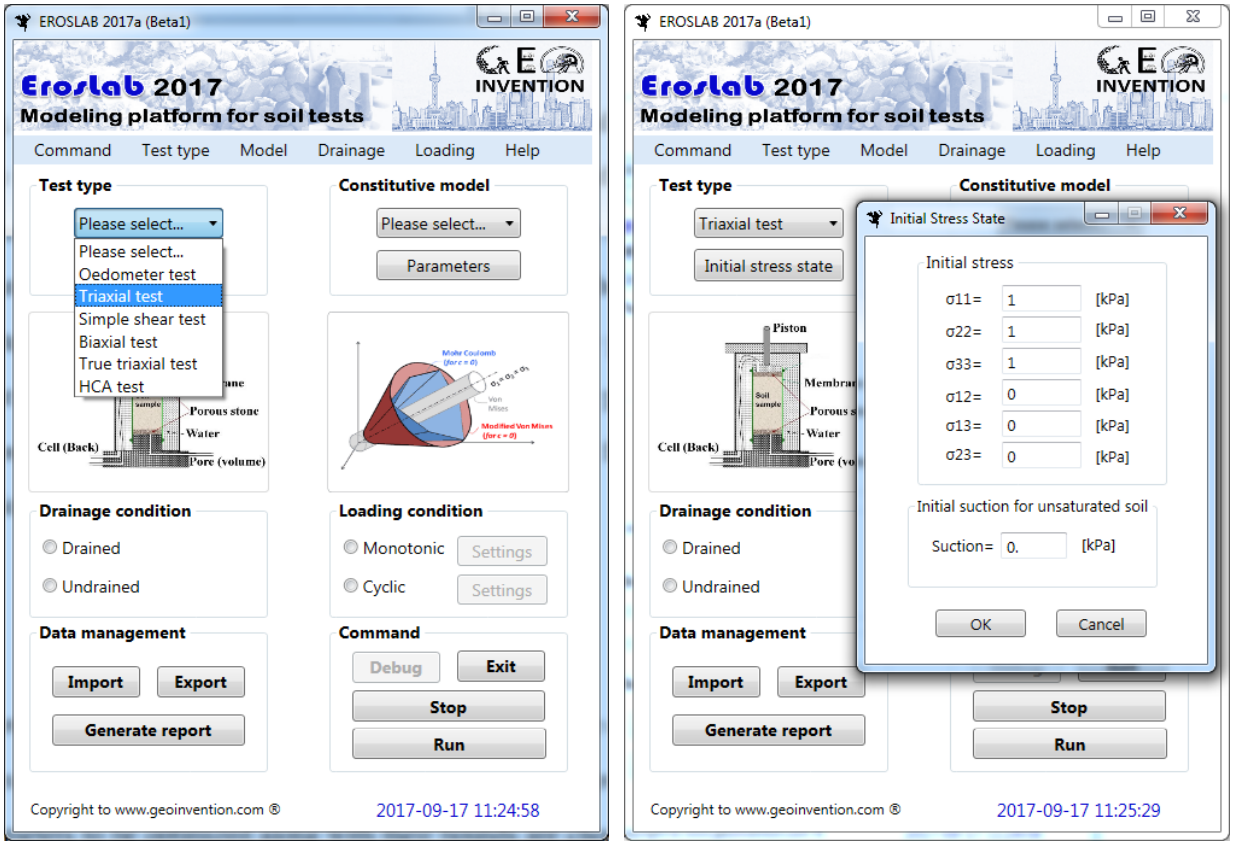
EROSLAB 2017a (Beta1)
Eroslab 2017
Modeling platform for soil tests
INVENTION
Command
Test type
Model
Drainage
Loading
Help
Test type
Please select...
Please select...
Oedometer test
Triaxial test
Simple shear test
Biaxial test
True triaxial test
HCA test
Constitutive model
Please select...
Parameters
Porous stone
Water
Cell (Back)
Drainage condition
Drained
Undrained
Loading condition
Monotonic
Settings
Cyclic
Settings
Data management
Import
Export
Generate report
Command
Debug
Exit
Stop
Run
Copyright to www.geoinvention.com ®
2017-09-17 11:24:58
EROSLAB 2017a (Beta1)
Eroslab 2017
Modeling platform for soil tests
INVENTION
Command
Test type
Model
Drainage
Loading
Help
Test type
Triaxial test
Initial stress state
Constitutive model
Initial Stress State
Initial stress
σ11= 1 [kPa]
σ22= 1 [kPa]
σ33= 1 [kPa]
σ12= 0 [kPa]
σ13= 0 [kPa]
σ23= 0 [kPa]
Initial suction for unsaturated soil
Suction= 0. [kPa]
OK
Cancel
Piston
Water
Cell (Back)
Drainage condition
Drained
Undrained
Data management
Import
Export
Generate report
Stop
Run
Copyright to www.geoinvention.com ®
2017-09-17 11:25:29

Figure 6

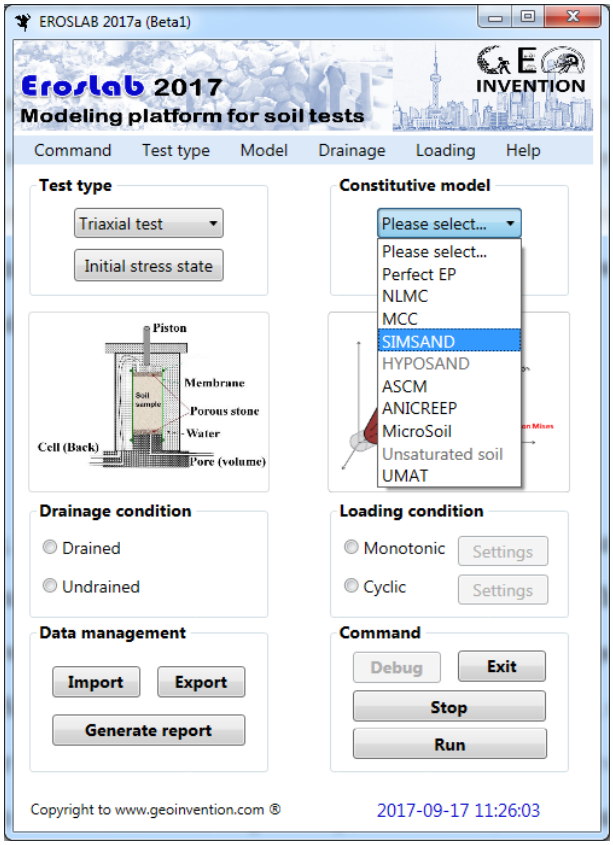
EROSLAB 2017a (Beta1)
Eroslab 2017
Modeling platform for soil tests
GEO INVENTION
Command
Test type
Model
Drainage
Loading
Help
Test type
Triaxial test
Initial stress state
Constitutive model
Please select...
Please select...
Perfect EP
NLMC
MCC
SIMSAND
HYPOSAND
ASCM
ANICREEP
MicroSoil
Unsaturated soil
UMAT
Piston
Membrane
Soil sample
Porous stone
Water
Cell (Back)
Pore (volume)
Drainage condition
Drained
Undrained
Loading condition
Monotonic
Settings
Cyclic
Settings
Data management
Import
Export
Generate report
Command
Debug
Exit
Stop
Run
Copyright to www.geoinvention.com ®
2017-09-17 11:26:03

(a)

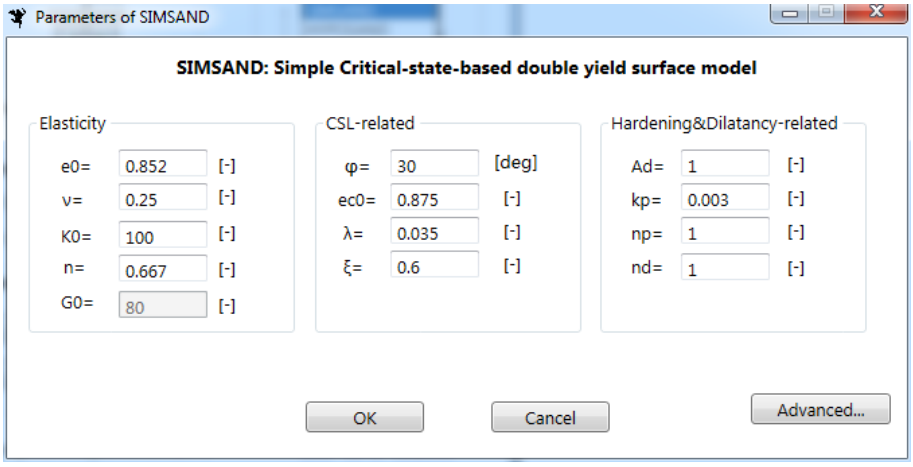
Parameters of SIMSAND
SIMSAND: Simple Critical-state-based double yield surface model
Elasticity
e0= 0.852 [-]
ν= 0.25 [-]
K0= 100 [-]
n= 0.667 [-]
G0= 80 [-]
CSL-related
φ= 30 [deg]
ec0= 0.875 [-]
λ= 0.035 [-]
ξ= 0.6 [-]
Hardening&Dilatancy-related
Ad= 1 [-]
kp= 0.003 [-]
np= 1 [-]
nd= 1 [-]
OK
Cancel
Advanced...

(b)

Figure 7

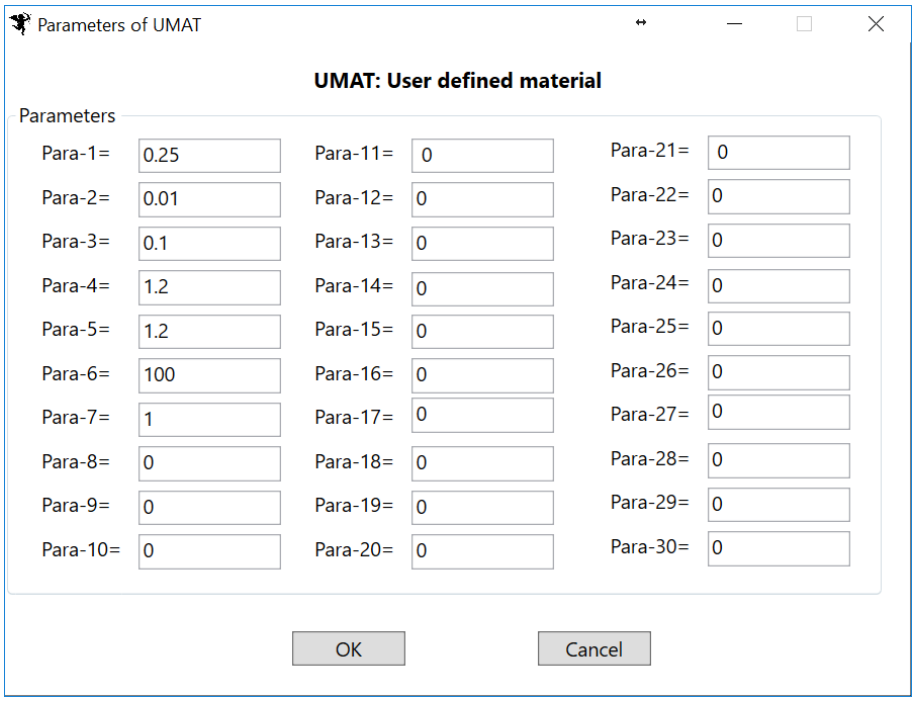
Parameters of UMAT
UMAT: User defined material
Parameters
Para-1= 0.25
Para-2= 0.01
Para-3= 0.1
Para-4= 1.2
Para-5= 1.2
Para-6= 100
Para-7= 1
Para-8= 0
Para-9= 0
Para-10= 0
Para-11= 0
Para-12= 0
Para-13= 0
Para-14= 0
Para-15= 0
Para-16= 0
Para-17= 0
Para-18= 0
Para-19= 0
Para-20= 0
Para-21= 0
Para-22= 0
Para-23= 0
Para-24= 0
Para-25= 0
Para-26= 0
Para-27= 0
Para-28= 0
Para-29= 0
Para-30= 0
OK
Cancel

Figure 8

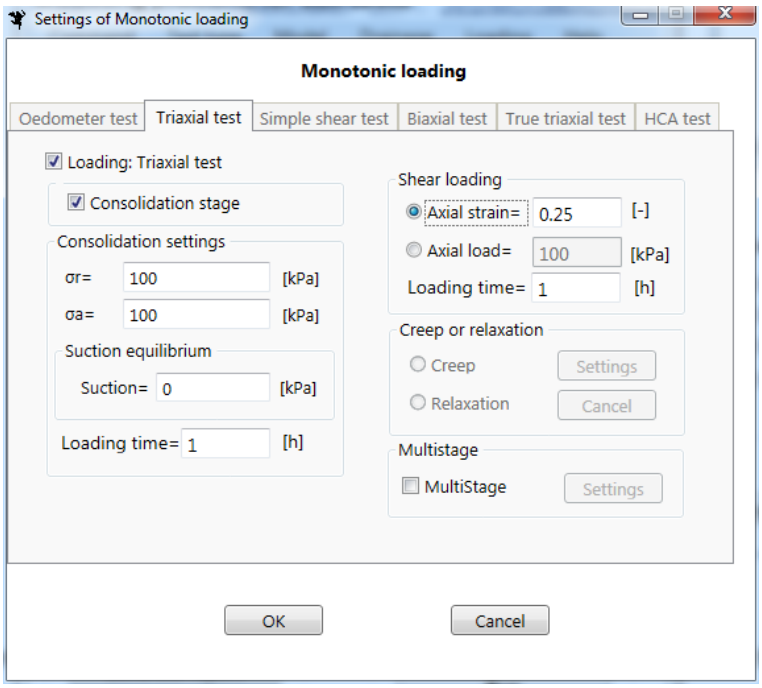
Settings of Monotonic loading
Monotonic loading
Oedometer test
Triaxial test
Simple shear test
Biaxial test
True triaxial test
HCA test
Loading: Triaxial test
Consolidation stage
Consolidation settings
σr= 100 [kPa]
σa= 100 [kPa]
Suction equilibrium
Suction= 0 [kPa]
Loading time= 1 [h]
Shear loading
Axial strain= 0.25 [-]
Axial load= 100 [kPa]
Loading time= 1 [h]
Creep or relaxation
Creep
Settings
Relaxation
Cancel
Multistage
MultiStage
Settings
OK
Cancel

Figure 9

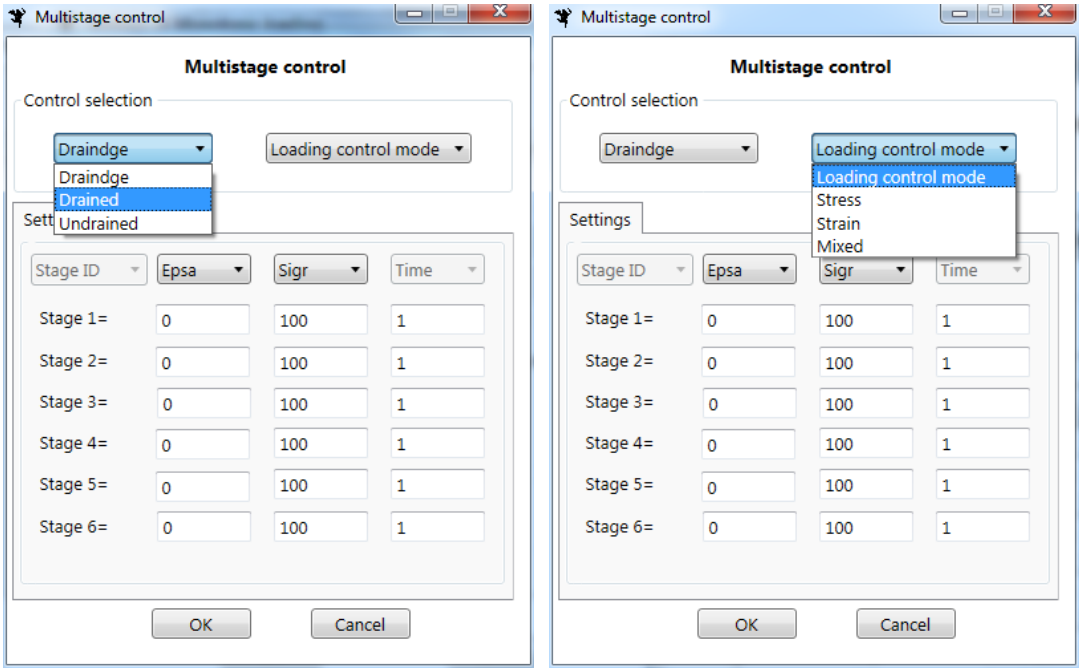
Multistage control
Multistage control
Control selection
Draindge
Loading control mode
Draindge
Drained
Undrained
Stage ID
Epsa
Sigr
Time
Stage 1=
Stage 2=
Stage 3=
Stage 4=
Stage 5=
Stage 6=
0
100
1
OK
Cancel
Multistage control
Multistage control
Control selection
Draindge
Loading control mode
Loading control mode
Stress
Strain
Mixed
Settings
Stage ID
Epsa
Sigr
Time
Stage 1=
Stage 2=
Stage 3=
Stage 4=
Stage 5=
Stage 6=
0
100
1
OK
Cancel

Figure 10

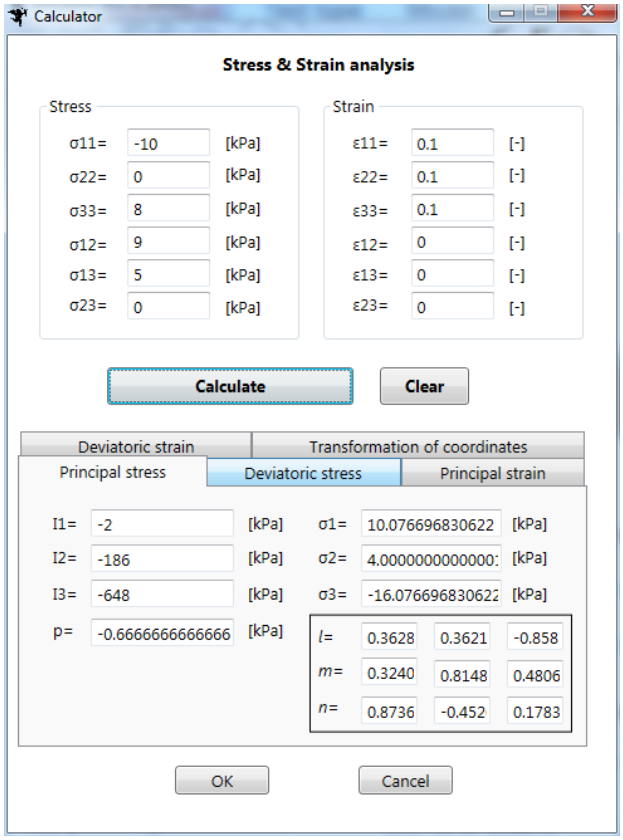
Calculator
Stress & Strain analysis
Stress
σ11= -10 [kPa]
σ22= 0 [kPa]
σ33= 8 [kPa]
σ12= 9 [kPa]
σ13= 5 [kPa]
σ23= 0 [kPa]
Strain
ε11= 0.1 [-]
ε22= 0.1 [-]
ε33= 0.1 [-]
ε12= 0 [-]
ε13= 0 [-]
ε23= 0 [-]
Calculate
Clear
Deviatoric strain
Transformation of coordinates
Principal stress
Deviatoric stress
Principal strain
I1= -2 [kPa]
I2= -186 [kPa]
I3= -648 [kPa]
p= -0.6666666666666 [kPa]
σ1= 10.076696830622 [kPa]
σ2= 4.0000000000000 [kPa]
σ3= -16.076696830622 [kPa]
l= 0.3628 0.3621 -0.858
m= 0.3240 0.8148 0.4806
n= 0.8736 -0.452 0.1783
OK
Cancel

Figure 11

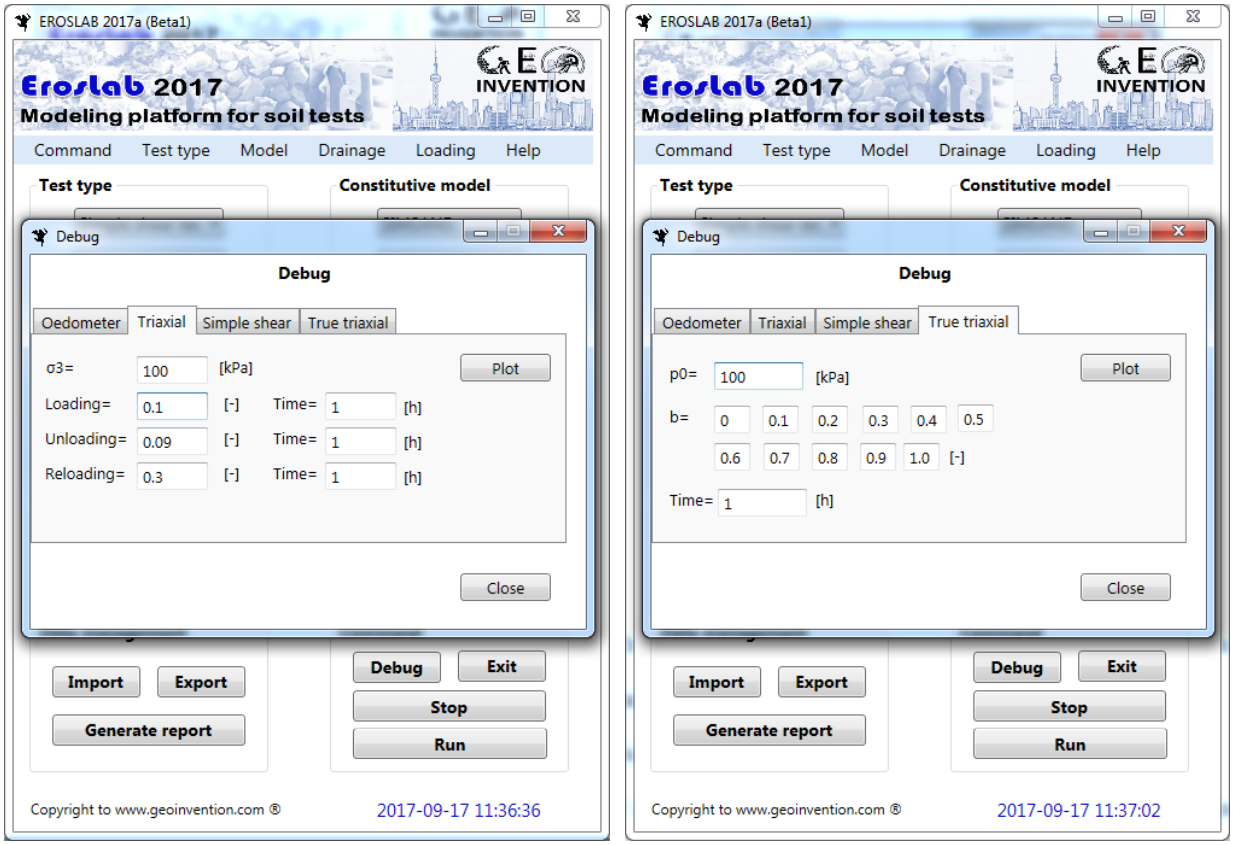
EROSLAB 2017a (Beta1)
Eroslab 2017
Modeling platform for soil tests
INVENTION
Command
Test type
Model
Drainage
Loading
Help
Test type
Constitutive model
Debug
Debug
Oedometer
Triaxial
Simple shear
True triaxial
σ3=
100
[kPa]
Plot
Loading=
0.1
[-]
Time=
1
[h]
Unloading=
0.09
[-]
Time=
1
[h]
Reloading=
0.3
[-]
Time=
1
[h]
Close
Import
Export
Generate report
Debug
Exit
Stop
Run
Copyright to www.geoinvention.com ®
2017-09-17 11:36:36
EROSLAB 2017a (Beta1)
Eroslab 2017
Modeling platform for soil tests
INVENTION
Command
Test type
Model
Drainage
Loading
Help
Test type
Constitutive model
Debug
Debug
Oedometer
Triaxial
Simple shear
True triaxial
p0=
100
[kPa]
Plot
b=
0
0.1
0.2
0.3
0.4
0.5
0.6
0.7
0.8
0.9
1.0
[-]
Time=
1
[h]
Close
Import
Export
Generate report
Debug
Exit
Stop
Run
Copyright to www.geoinvention.com ®
2017-09-17 11:37:02

Figure 12

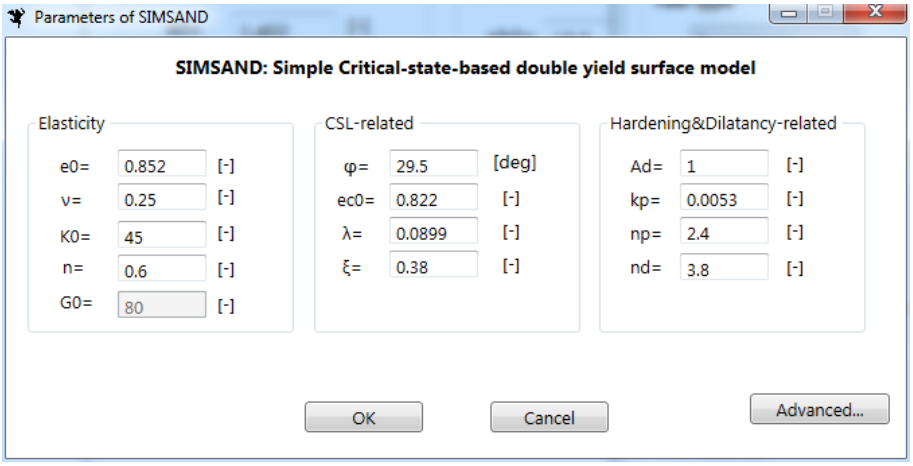
Parameters of SIMSAND
SIMSAND: Simple Critical-state-based double yield surface model
Elasticity
e0= 0.852 [-]
ν= 0.25 [-]
K0= 45 [-]
n= 0.6 [-]
G0= 80 [-]
CSL-related
φ= 29.5 [deg]
ec0= 0.822 [-]
λ= 0.0899 [-]
ξ= 0.38 [-]
Hardening&Dilatancy-related
Ad= 1 [-]
kp= 0.0053 [-]
np= 2.4 [-]
nd= 3.8 [-]
OK
Cancel
Advanced...

Figure 13

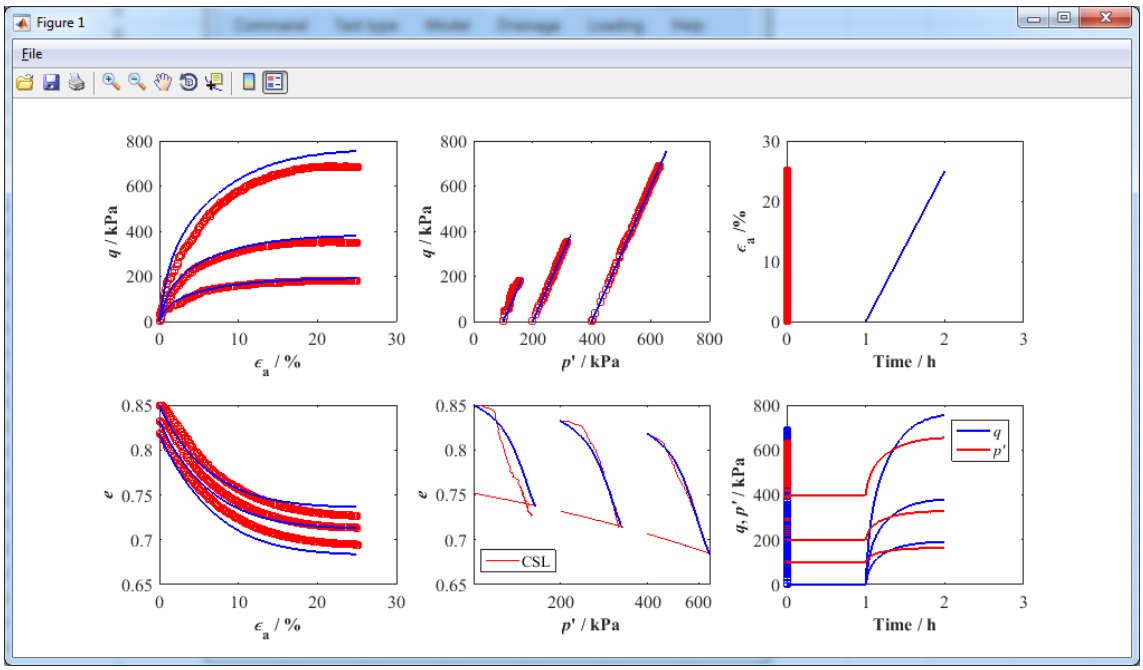
Figure 1
File
q / kPa
ϵa / %
p' / kPa
Time / h
e
CSL
q, p' / kPa
q
p'

(a)

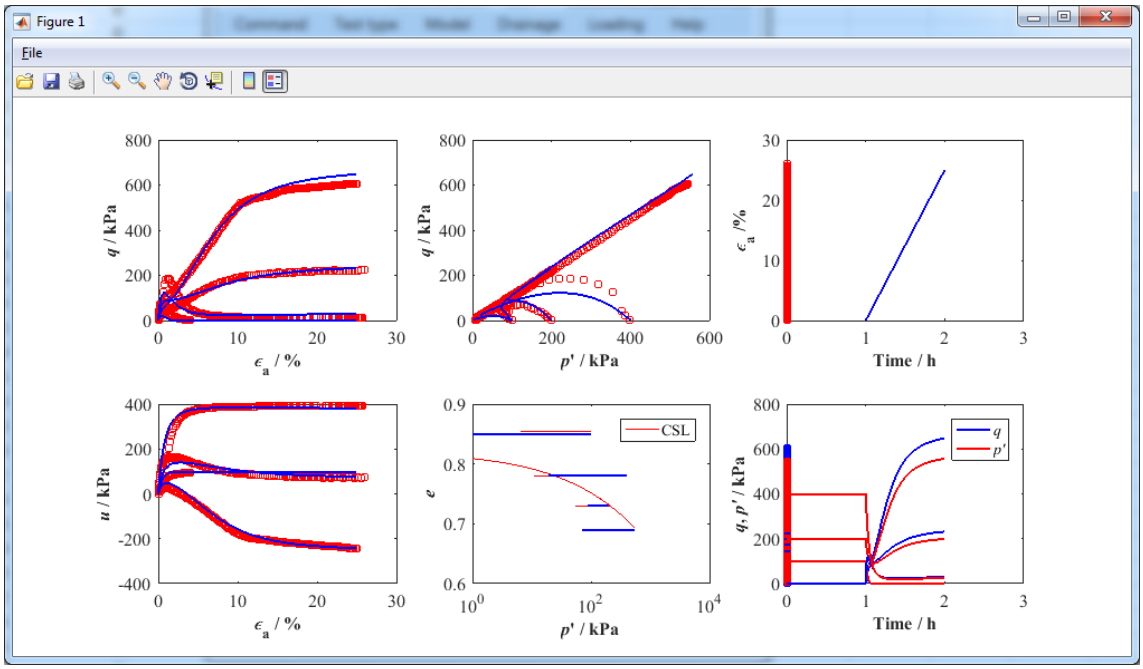
Figure 1
File
q / kPa
ϵa / %
p' / kPa
Time / h
u / kPa
e
CSL
q, p' / kPa
q
p'

(b)

Figure 14

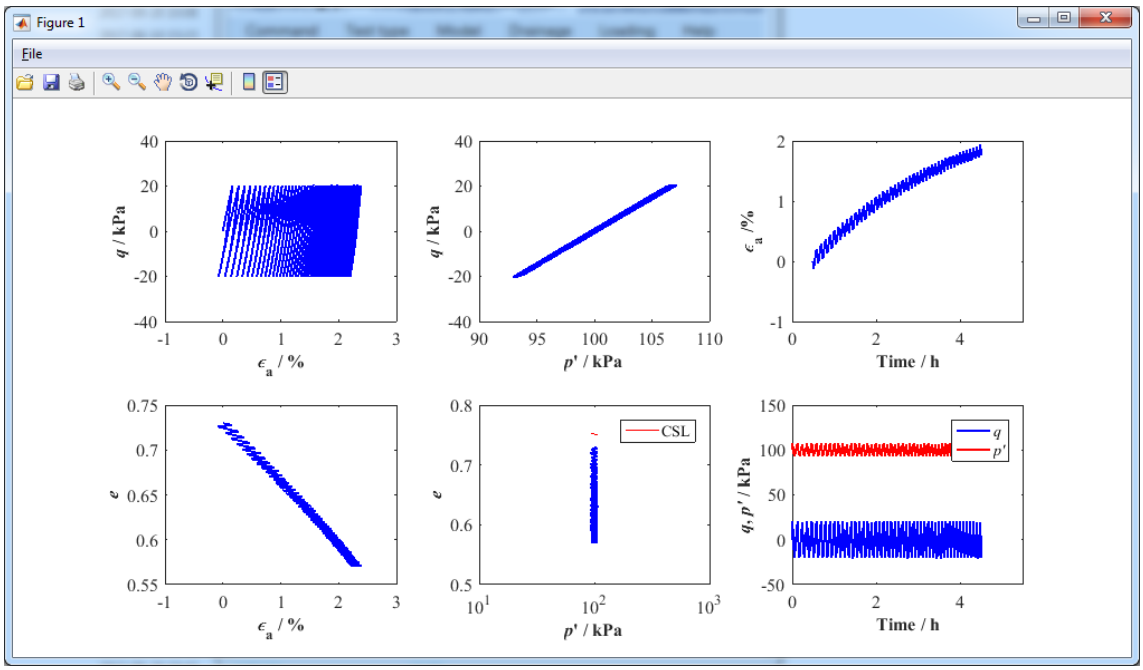
Figure 1
File
q / kPa
ϵa / %
p' / kPa
ϵa /%
Time / h
e
CSL
q, p' / kPa
q
p'

(a)

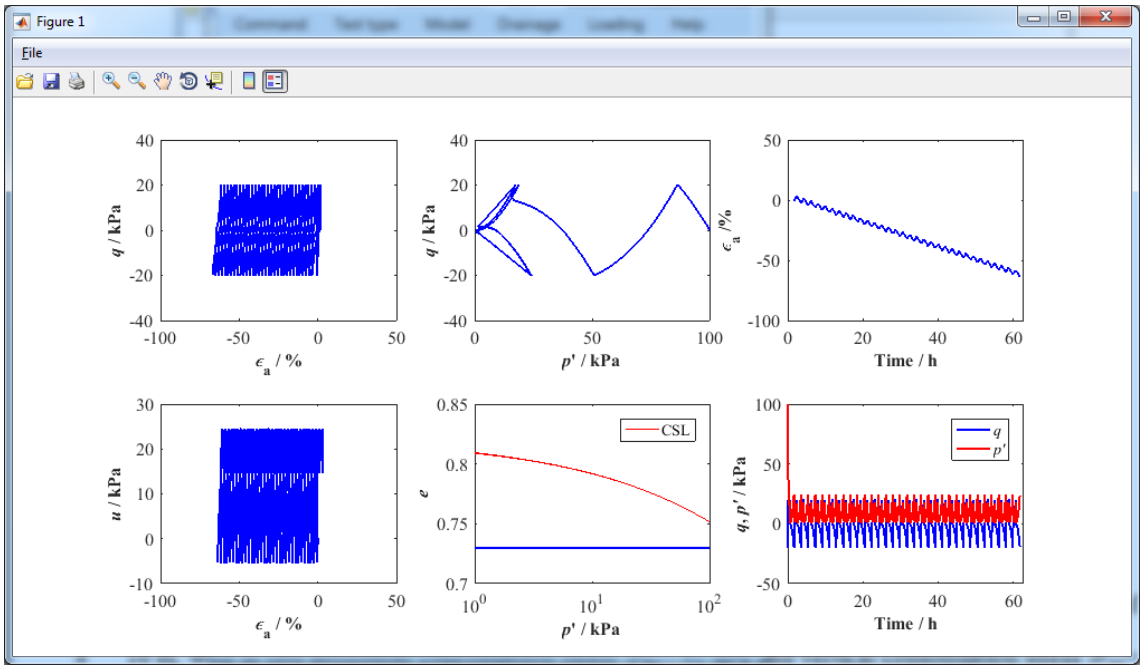
Figure 1
File
q / kPa
ϵa / %
p' / kPa
ϵa /%
Time / h
u / kPa
e
CSL
q, p' / kPa
q
p'

(b)

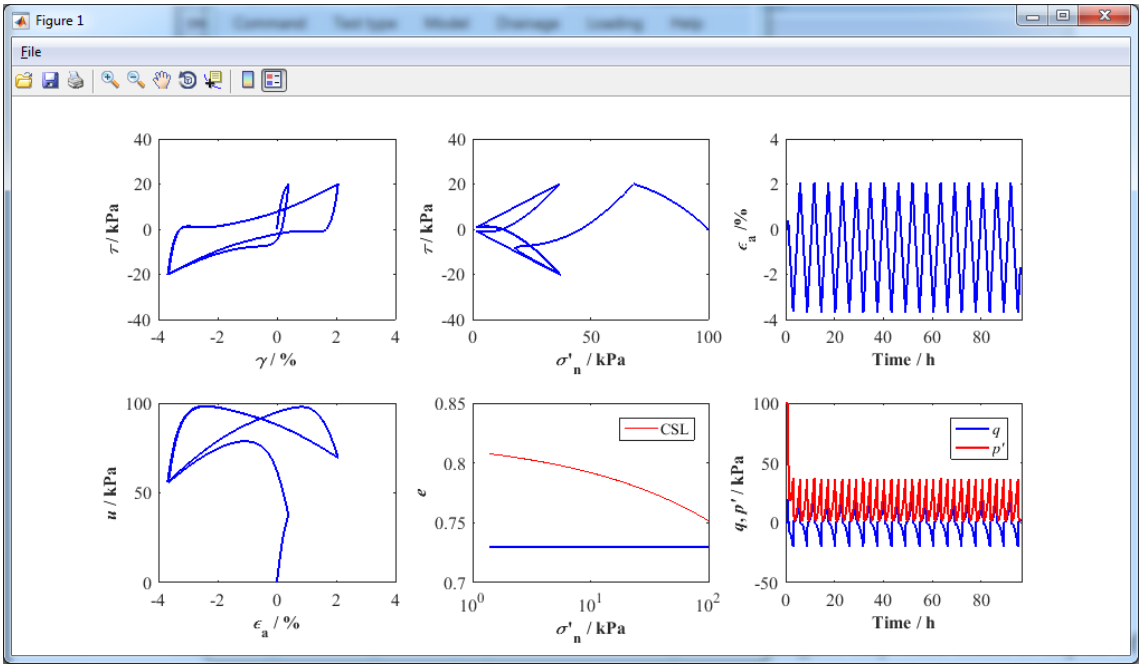
Figure 1
File
τ / kPa
γ / %
τ / kPa
σ'n / kPa
ϵa /%
Time / h
u / kPa
ϵa / %
e
CSL
σ'n / kPa
q, p' / kPa
q
p'
Time / h

(c)

Figure 15

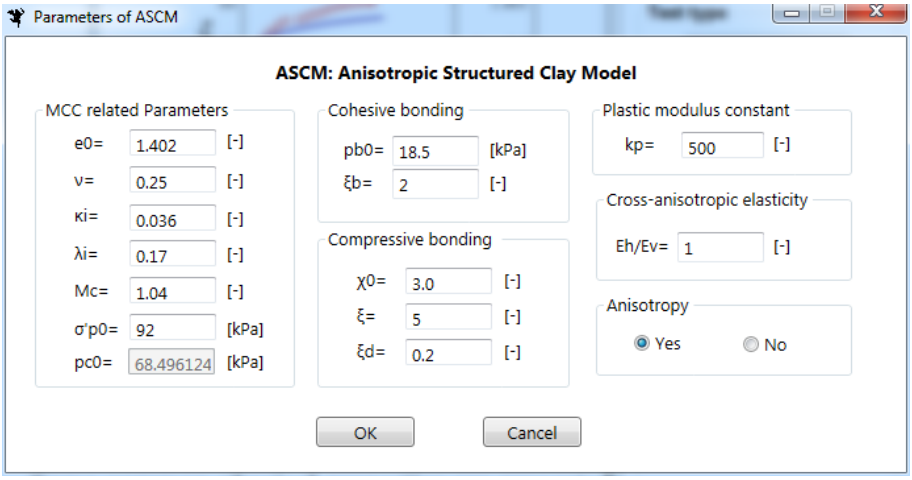
Parameters of ASCM
ASCM: Anisotropic Structured Clay Model
MCC related Parameters
e0= 1.402 [-]
ν= 0.25 [-]
κi= 0.036 [-]
λi= 0.17 [-]
Mc= 1.04 [-]
σ'p0= 92 [kPa]
pc0= 68.496124 [kPa]
Cohesive bonding
pb0= 18.5 [kPa]
ξb= 2 [-]
Compressive bonding
χ0= 3.0 [-]
ξ= 5 [-]
ξd= 0.2 [-]
Plastic modulus constant
kp= 500 [-]
Cross-anisotropic elasticity
Eh/Ev= 1 [-]
Anisotropy
Yes
No
OK
Cancel

Figure 16

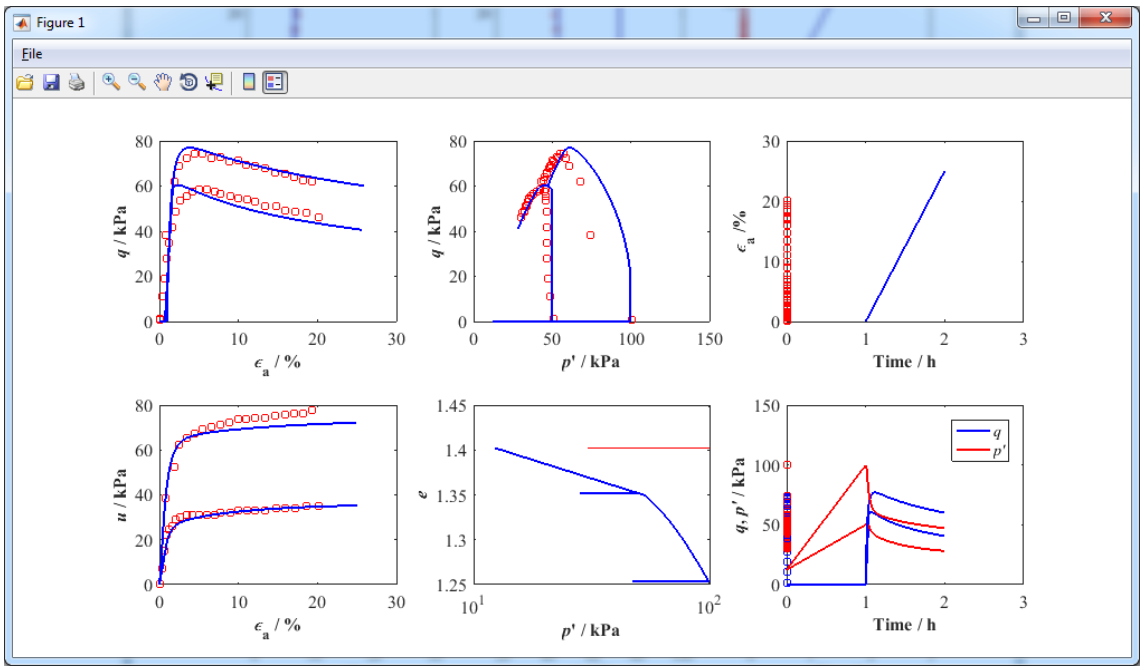
Figure 1
File
q / kPa
ϵa / %
p' / kPa
ϵa /%
Time / h
u / kPa
e
q, p' / kPa
q
p'

(a)

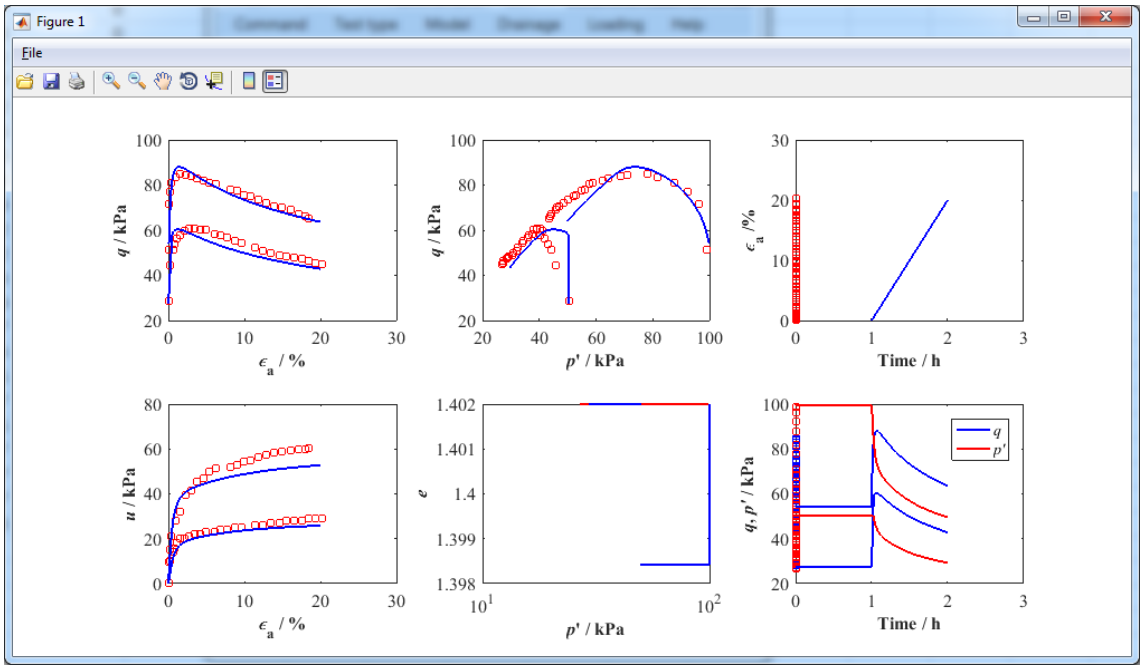
Figure 1
File
q / kPa
ϵa / %
p' / kPa
ϵa /%
Time / h
u / kPa
e
q, p' / kPa
q
p'

(b)

Figure 17

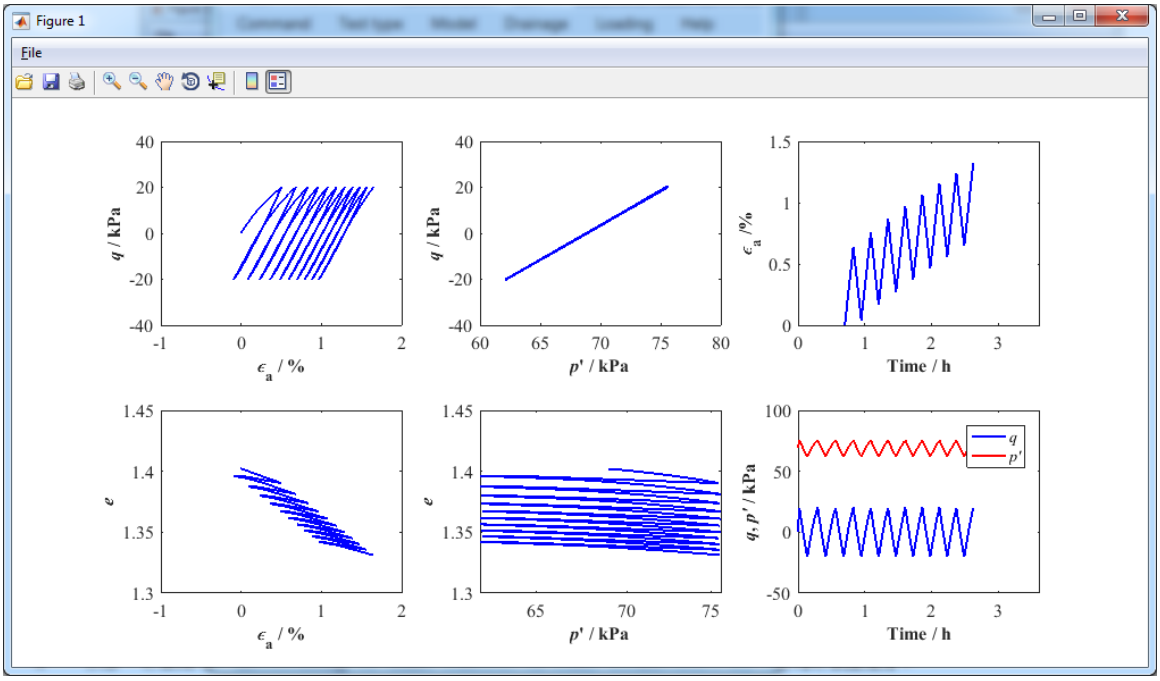
Figure 1
File
q / kPa
ϵa / %
p' / kPa
ϵa /%
Time / h
e
q, p' / kPa
q
p'
u / kPa

(a)

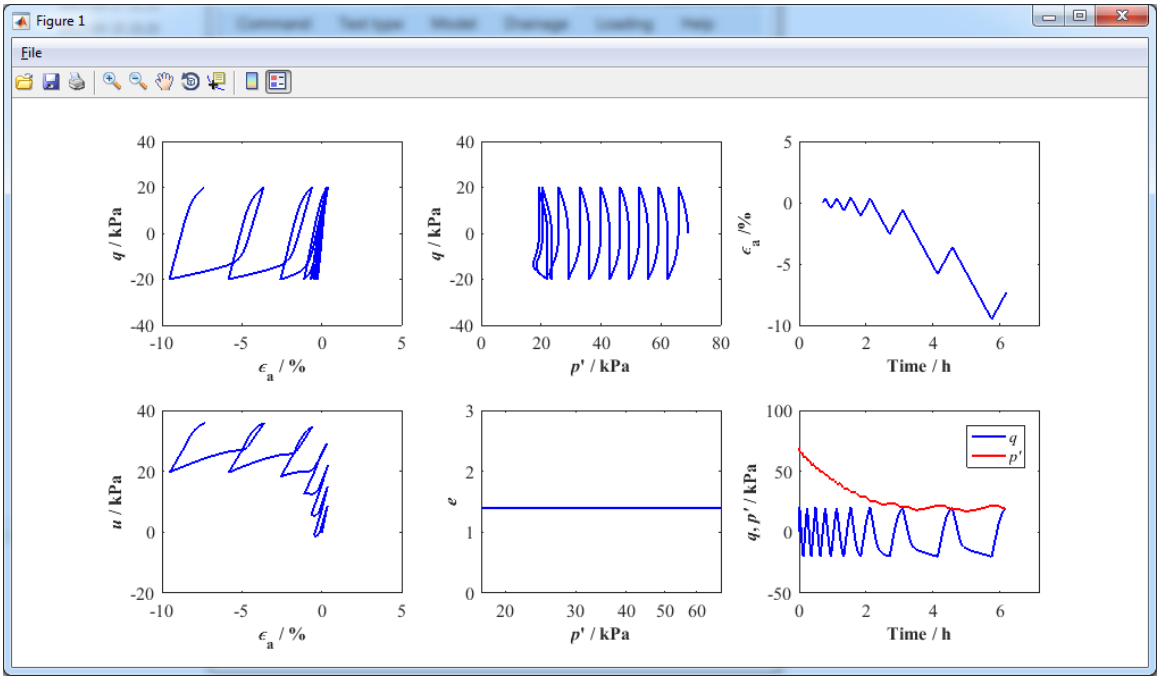
Figure 1
File
q / kPa
ϵa / %
p' / kPa
ϵa /%
Time / h
u / kPa
e
q, p' / kPa
q
p'

(b)

Figure 18

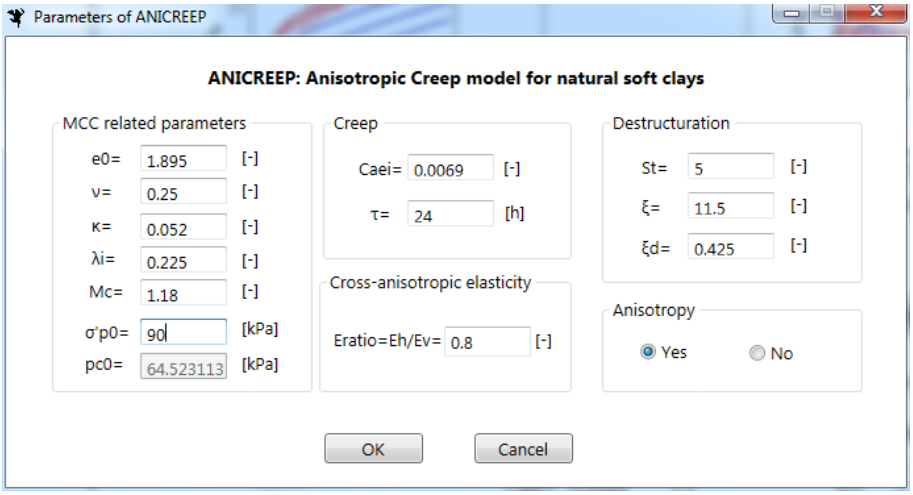
Parameters of ANICREEP
ANICREEP: Anisotropic Creep model for natural soft clays
MCC related parameters
e0= 1.895 [-]
v= 0.25 [-]
κ= 0.052 [-]
λi= 0.225 [-]
Mc= 1.18 [-]
σ'p0= 90 [kPa]
pc0= 64.523113 [kPa]
Creep
Caei= 0.0069 [-]
τ= 24 [h]
Cross-anisotropic elasticity
Eratio=Eh/Ev= 0.8 [-]
Destructuration
St= 5 [-]
ξ= 11.5 [-]
ξd= 0.425 [-]
Anisotropy
Yes
No
OK
Cancel

Figure 19

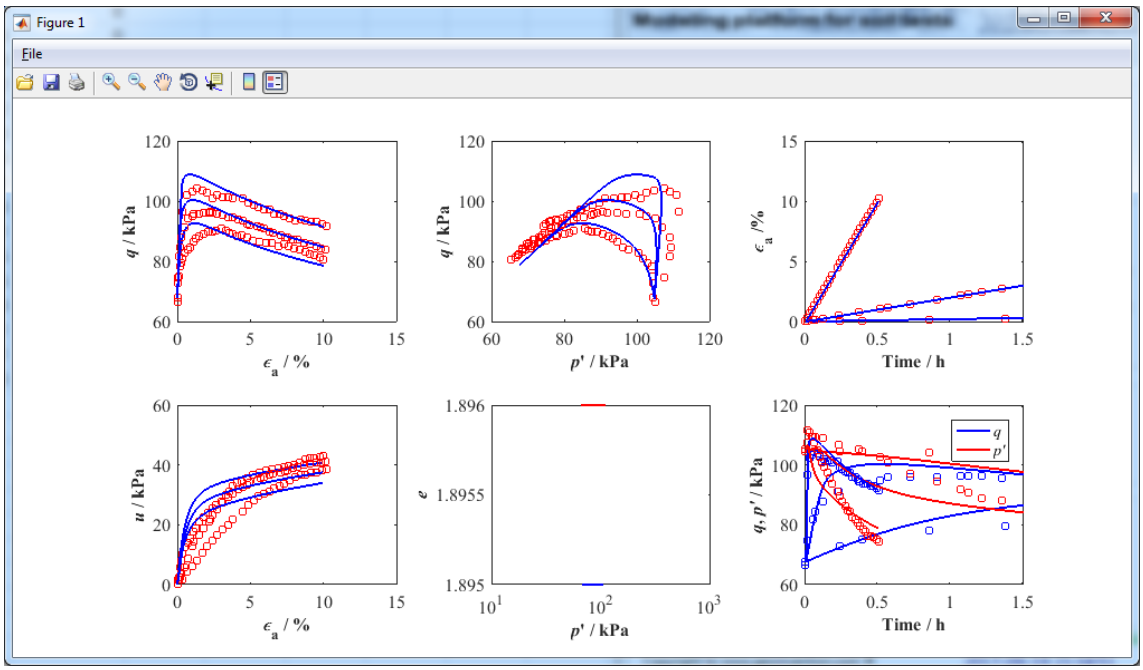
Figure 1
File
q / kPa
ϵa / %
p' / kPa
Time / h
u / kPa
e
q, p' / kPa
q
p'

(a)

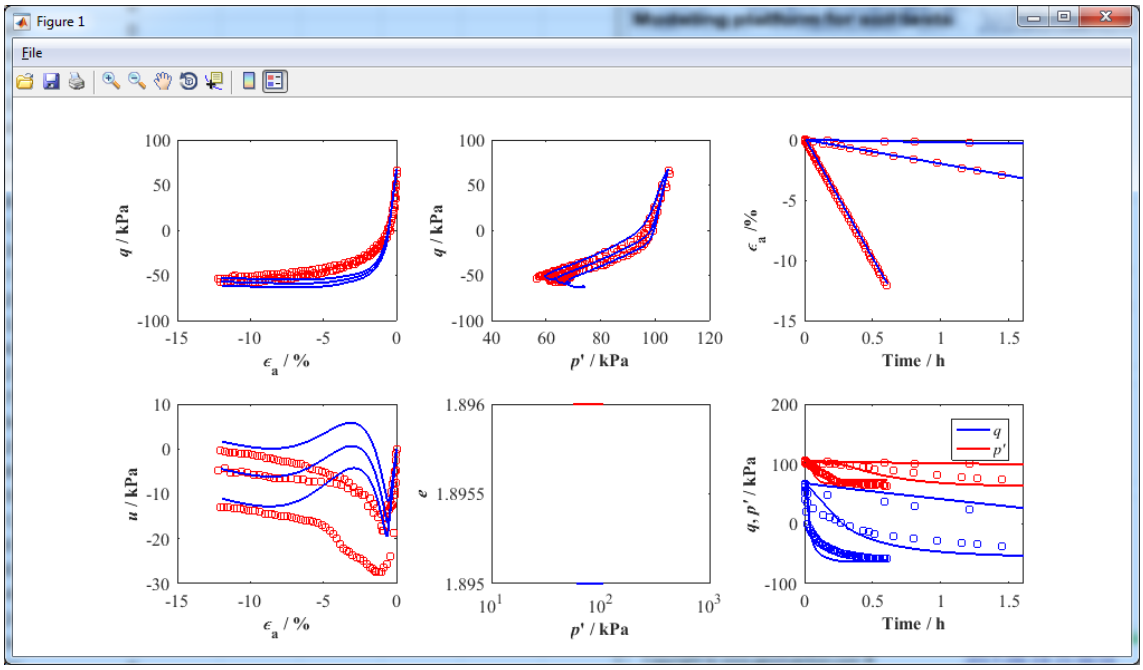
Figure 1
File
q / kPa
ϵa / %
p' / kPa
Time / h
u / kPa
e
q, p' / kPa
q
p'

(b)